The family of *Pseudo Response Regulator* genes (*PRR*) in the moss *Physcomitrella patens*.

SANTOSH BALASAHEB SATBHAI

ACKNOWLEDGEMENTS

Firstly, I wish to thank my supervisor Dr. Setsuyuki Aoki for his constant guidance, support and intellectual input throughout my PhD studies. I wish to thank Japanese Government for awarding Monbukagakusho-MEXT scholarship that supported this work. I am also grateful to Prof. Mizuno for his financial support during final stage of my PhD. Also, without the collaboration of Dr. Aoki group and Prof. Mizuno group, this work could not have been completed. Thanks also to Prof. Mizuno again and Dr. Yamashino for their interests in my research project.

Thank you to the members of the Aoki Laboratory, and the *Arabidopsis* Laboratory (Prof. Mizuno group), for their assistance, advice and friendship over the last four years. In particular, I would like to thank Dr. Yamashino, who spent many patient hours teaching me about working with *Arabidopsis*, who developed many of the protocols for analysis of the transgenic plants, and who was the pioneer for much of the work performed as part of my research. I would like to also thank to Prof. Yoshida, Dr. Tsukamoto, and Dr. Nakagawa for their moral support. I would also like to thank my friend Dr. Sudhir Landge for his kind guidance and support before and during my PhD research.

Finally, I would like to give a special thanks to my family and friends, without whom I would never have made it this far. Thanks for all your love and support, and for always believing in me.

CONTENTS

LIST OF FIGURES

LIST OF TABLES

ABBREVIATIONS

A. thaliana	*Arabidopsis thaliana*
A. tumefaciens	*Agrobacterium tumefaciens*
ACT	*Actin*
ATP	adenosine tri phosphate
bp	basepair
BLAST	basic local alignment search tool
BRASS	Biological Rhythm Analysis Software System
BSA	bovine serum albumin
CAB	*Chlorophyll A/B binding*
$CaCl_2$	calcium chloride
CaMV	Cauliflower Mosaic Virus
CCA1	*Circadian Clock Associated 1*
CCR2	*Cold-Circadian Rhythm RNA Binding 2*
Col	Columbia
CCT	CO, CO-like and TOC1
cDNA	complementary deoxyribonucleic acid
CO	CONSTANS
COL	CONSTANS-like
CRY1-2	*CRYPTOCHROME 1-2*
DD	continuous dark
DNA	deoxyribonucleic acid
DNase	deoxyribonuclease 1
DTT	dithiothreitol
E. coli	*Escherichia coli*
EDTA	ethylene diamine tetraacetic acid
GI	*GIGANTEA*
HCl	hydrochloric acid
HK	*Histidine Kinase*

Hpt/HP	histidine containing phospho-transmitter
HR	homologous recombination
IPTG	isopropyl β-D-thiogalactopyranoside
kb	kilobasepair
KCl	potassium chloride
kDa	kiloDaltons
LD	light-dark
LED	light emitting diode
Lhcb	*light harvesting chlorophyll A/B binding*
LHY	*Late Elongated Hypocotyl*
LL	continuous light
LUC	*Luciferase*
$MgCl_2$	magnesium chloride
Mpa	megapascals
mRNA	messenger ribonucleic acid
MS	Murashige and Skoog
MW	molecular weight
Mya	million years ago
nm	nanometer
PAGE	polyacrylamide gel electrophoresis
PCR	polymerase chain reaction
PEG	polyethylene glycol
PHY	*PHYTOCHROME*
P. patens	*Physcomitrella patens*
PRR	*Pseudo Response Regulators*
qRT-PCR	quantitative real-time PCR
RR	Response Regulators
RNA	ribonucleic acid
RNase	ribonulease A
rpm	rotations per minute
RT	room temperature

RLD	Receiver Like domain
RT-PCR	reverse transcribed polymerase chain reaction
SDS	sodium dodecyl sulphate
sqRT-PCR	semi-quantitative reverse-transcription PCR
TOC1	*Timing of CAB Expression 1*
UTR	untranslated region
WT	wild type
ZT	zeitgber time
ZTL	*Zeitlupe*

1. INTRODUCTION

1.1 A basic model of circadian system

Circadian rhythms are endogenous, self generating cycles of a ~ 24-hour period that are found in organisms, from cyanobacteria to plants and animals (Dunlap, 1999). In simplified conceptual model, the circadian system, that underpins expression of circadian rhythms, has been divided into three main components: the *input pathways* involved in the perception and transmission of environmental signals to synchronize the *central oscillator* or *circadian clock* that generates and maintains rhythmicity through multiple *output pathways* that connect the oscillator to physiology and metabolism (Fig. 1). Recently, several lines of evidence reveal the existence of a far more complicated circadian system, with output elements modulating the pace of the oscillator and input elements being themselves tightly controlled by the clock (McClung, 2001; Mas, 2005).

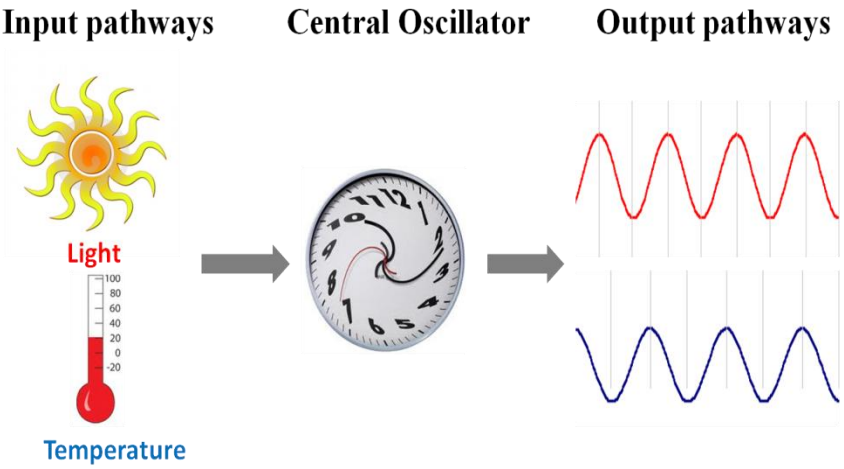

Figure 1. Organization of the circadian system.

Input pathways, such as light and temperature, connect the clock with the external environment. Central oscillator is machinery that generates self-sustained oscillation. Output from the oscillators produces rhythms that can differ in phase. Adapted from McClung (2001) and Más (2005).

The primary role of the circadian clock is to adjust the timing of metabolism, physiology and behavior of organisms, coordinating them to environmental factors that cycle with the rotation of the earth (Edmunds, 1988; Pittendrigh, 1993). In various model organisms, molecular genetic studies have led to the isolation of a repertoire of genes with important functions in the generation of the clock oscillation; in particular, essential ones are collectively called "clock genes" (Hamilton and Kay, 2008). The mechanisms of the eukaryotic clocks are proposed to be founded on interlocked auto-regulatory loops between these genes, while the identities of these genes are in principle different between animals, plants and fungi (Hamilton and Kay, 2008).

1.2 The *Arabidopsis* circadian clock

In higher plants, the circadian clock regulates a wide range of biological processes, including leaf movement, stomatal opening, photosynthesis, photoperiodic control of flowering time, growth and development (Barak *et al.*, 2000, McClung, 2001). Molecular mechanisms underlying plant circadian rhythms have been extensively studied in the model dicot *Arabidopsis thaliana* (*A. thaliana*). Approximately 2–16% of the genes expressed in *A. thaliana* have circadian rhythms in the steady-state levels of transcript abundance largely as output effectors or intermediate regulators (Harmer *et al*. 2000; Schaffer *et al*. 2001; Edwards *et al*. 2006). In *A. thaliana*, moreover, many genes have been identified to be involved in the core clock mechanism (Hamilton and Kay, 2008; Harmer, 2009). A representative set of such genes is the *Pseudo-Response Regulator* (*PRR*) gene family, which comprises five member genes, *TOC1* (also called *PRR1*)*/PRR3/PRR5/PRR7/PRR9*. These *PRR* genes have been shown to play regulatory roles at multiple nodes in the interlocked loops of the *A. thaliana* circadian network (Mizuno and Nakamichi, 2005; Harmer, 2009; Fig. 2). In a putative core loop (loop A in Fig. 2), a pair of single myb transcription factors, Circadian Clock-Associated 1 (CCA1) and its paralog Late elongated HYpocotyl (LHY) repress *TOC1* expression, while TOC1 protein activates *CCA1/LHY* expression (Alabadí *et al*., 2001). CCA1/LHY are coupled with a second loop, where they activate a pair of *PRR* members, *PRR7* and *PRR9* (and possibly *PRR5* as well, loop C in Fig. 2),

while the protein product of these genes in turn repress *CCA1/LHY* to close the loop (Farre *et al*., 2005; Nakamichi *et al*., 2010). It is proposed that TOC1 represses a yet unidentified factor, which in turn activates *TOC1* in a third loop (Locke *et al*., 2006; Zeilinger *et al*., 2006, loop B in Fig. 2). Additionally, PRR3 stabilizes TOC1 by interfering with the binding between TOC1 and Zeitlupe (ZTL), the latter of which is an F-box protein that recruits TOC1 for proteasomal degradation (Más *et al*, 2003; Para *et al*., 2007; Fujiwara *et al*., 2008, loop D in Fig. 2). All the *PRR* genes are, largely based on phenotypic analyses of mutants, supposed to be functionally important in the *A. thaliana* circadian system (Harmer, 2009). Although phenotypic changes of a single mutation of each *PRR* gene are not large, combinations of mutations of different *PRRs* often result in stronger phenotypes, *e.g.*, essentially arrhythmic in an extreme case (Harmer, 2009).

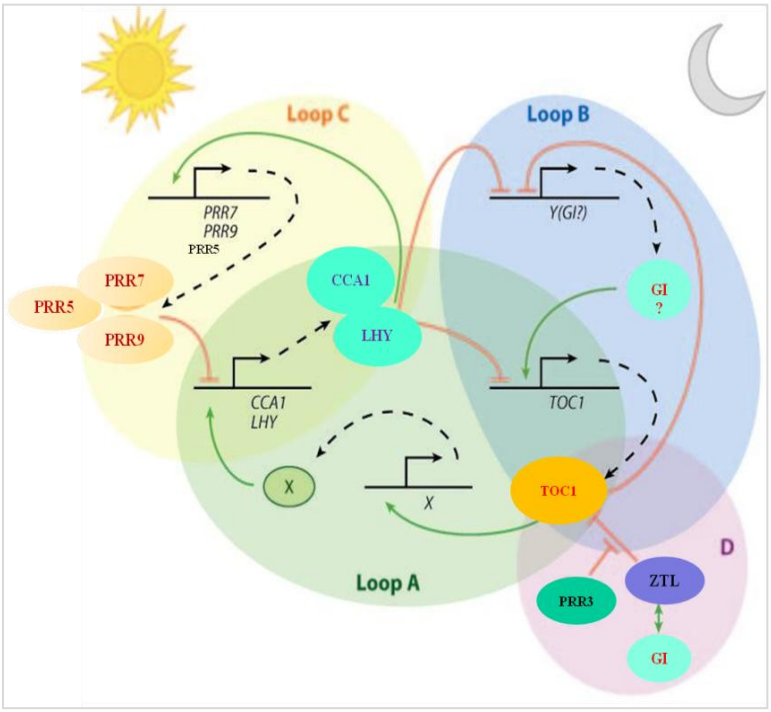

Figure 2. Model of the *A. thaliana* circadian clock. The circadian oscillator consists of a series of interlocking feedback loops. Three feedback loops (loops A - C) form a transcriptional network that regulates clock function. Moreover, essential to clock function are post-transcriptional regulatory mechanisms (loop D). Adapted from Harmer (2009).

1.3 Evolution of PRRs is a mystery

PRRs share two conserved domains, a receiver-like domain (RLD) and a CONSTANS/CONSTANS-LIKE/TOC1 (CCT) domain at their amino- and carboxy-termini, respectively. This CCT motif is a plant-specific motif that is found in many apparently unrelated plant proteins, including a photoperiodic regulator CONSTANS and its paralog proteins CONSTANS-LIKEs, and it contains a nulclear-localization signal (Mizuno and Nakamichi, 2005). On the other hand, RLD is similar to the receiver domain of the response regulators (RRs) in the histidine to aspartic acid (His-Asp) phosphorelay, which is a versatile signal transduction system broadly observed in organisms from bacteria to eukaryotes other than animals (Mizuno, 2005; Mizuno and Nakamichi, 2005). The RRs were originally discovered as common components of the His-Asp phosphorelay in prokaryotes. Through the course of evolution, higher plants have also come to employ such prokaryotic RRs for their own signal transduction, such as the elicitation of plant hormone (*e.g.*, cytokinin) responses (Fig. 3).

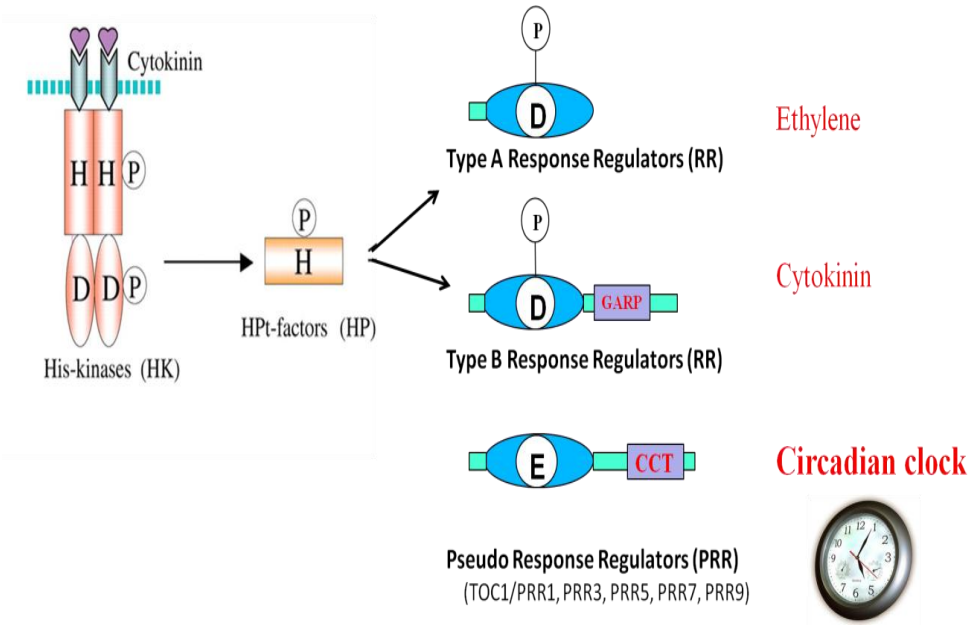

Figure 3. A schematic representation of the structural features of plant His-Asp phosphorelay-associated signal transduction components. Histidine kinases (HKs; *e.g.*,

cytokinin receptors) consist of three domains: N-terminal sensor domain (*e.g.*, cytokinin-binding domain), central HK domain containing an invariant phospho-accepting histidine (H) residue, and C-terminal receiver domain containing an invariant aspartic acid (D) residue, which is capable of accepting a phosphate group from a phospho-histidine. The phosphate group on the receiver domain is transferred to a histidine containing phospho-transmitter (HPt or HP), which subsequently serves as a phospho-donor toward an RR, which triggers downstream events that are responsive to a specific signal, such as plant hormones ethylene and cytokinin. Also shown is an atypical RR termed as Pseudo Response Regulator (PRR) in which invariant D is replaced by E (glutamic acid). Adapted from Ishida *et al*. (2009).

In the His-Asp phosphorelay, a phosphate group is transferred from a histidine kinase (HK), via an intermediate signal transducer histidine-containing phosphotransmitter (HPt), down to a counterpart RR, thereby transducing various environmental and endogenous signals intracellularly (Fig. 3; Mizuno, 2005). It is well known that an aspartic acid residue of the receiver domain is conserved as the phosphoacceptor site (Mizuno, 2005). Interestingly, RLDs of all the PRRs so far identified from flowering plants lack the aspartic acid residue for this phosphotransfer function, and they carry a glutamic acid instead (Mizuno, 2005; Mizuno and Nakamichi, 2005). Consistent with this, Makino *et al*. (2000) showed that the RLD of TOC1 did not undergo phosphotransfer *in vitro*. No attempt has so far been made to elucidate the evolutionary relationships between RRs and PRRs. Therefore, biochemical functions of PRRs and their evolutionary origins have been a mystery to date.

Homolog sequences of the *A. thaliana* clock genes have recently been characterized in several other flowering plants (Murakami *et al*. 2003; Hecht *et al*. 2005; Ramos *et al*. 2005; Miwa *et al.* 2005; Ishida *et al*. 2008; Liu *et al*. 2009; Takata *et al*. 2010). The consensus result of these studies is that homologs to core clock genes in *A. thaliana* are present and furthermore appear to display a high degree of functional conservation. PRRs are also well conserved in flowering plants, and they all lack the aspartic acid residue that is invariably found in authentic RRs. On the other hand, there have been so few studies of PRR homolog sequences in non-flowering plant groups, which cover a wide spectrum of plant species. Therefore, in order to understand the diversity and evolution of PRRs, related sequences should be characterized in lower plant (non-flowering plant) species, especially in phylogenetically basal groups of plants.

1.4 *Physcomitrella patens* as a model plant

Physcomitrella patens (*P.patens*) is a species of Bryopsida (moss), one of the basal land plants (Bowman et al., 2007; Lang *et al*., 2008), diverged from flowering plant lineages at least 450 million years ago (Lang *et al*., 2008, Fig. 4). In common with ferns and flowering plants, mosses show alternation of generations: a haploid phase that produces gametes (the gametophyte generation) and a diploid phase that produces haploid spores by meiosis (the sporophyte generation).

The life cycle of moss can be depicted briefly as follows. Spores germinate to produce the protonemal stage of the gametophyte. The protonema consists of a filamentous network of chloroplast rich chloronemata, and caulonemata that contain relatively few chloroplasts. The second tissue is the mature gametophore or leafy shoot, which differentiates from a bud-like apical meristem that formed on caulonemata (Schaefer and Zrÿd, 2001). Gametophores produce leaf-like structures called leaflets, consisting of a single cell layer, and root-like structures called rhizoids (Fig. 5). Gametophores also carry the reproductive organs of moss and support the formation of diploid sporophyte following fertilization. The entire life cycle can be completed in ~3 months in culture.

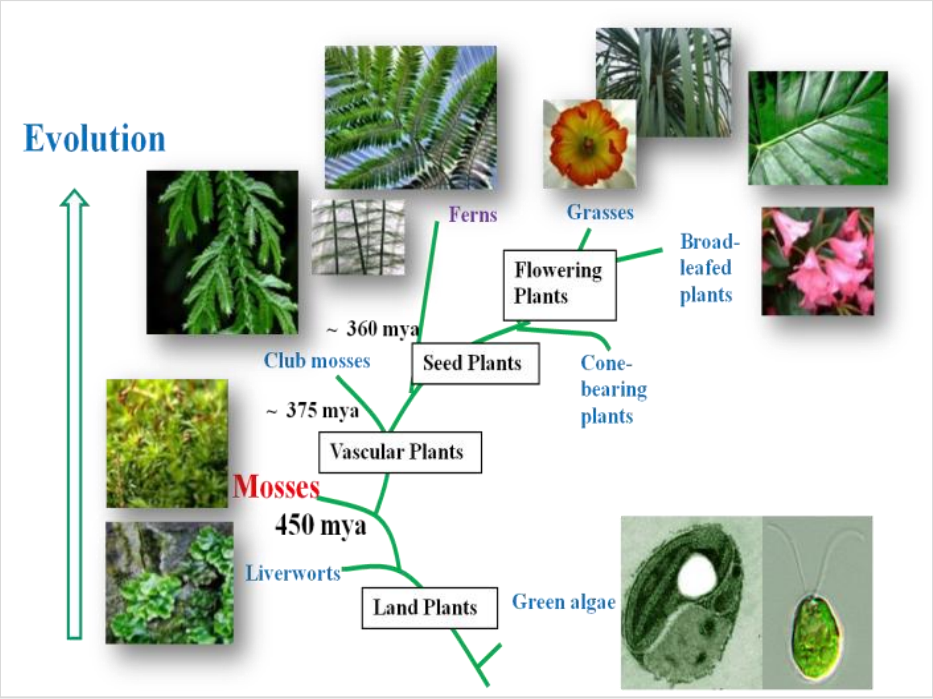

Figure 4. Evolutionary relationships (diversity) among green plants: Mosses are at a basal position in land plant evolution (mya= million years ago). Adapted from *Plant Cell* teaching tools (http://www.plantcell.org/teachingtools/teaching.dtl).

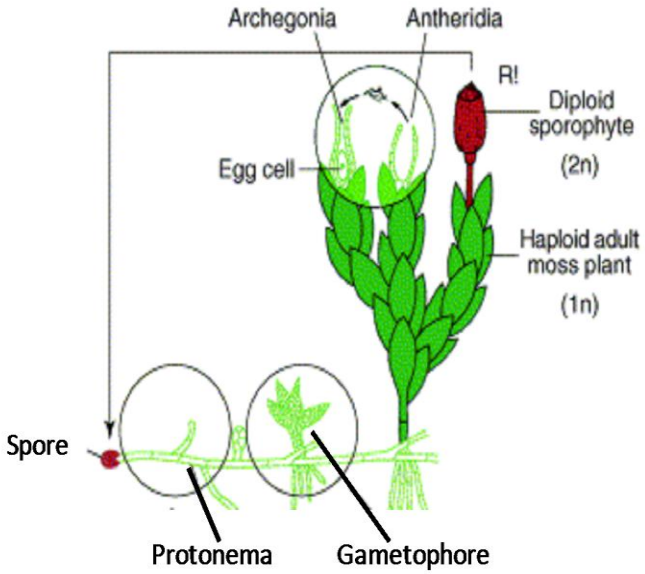

Figure 5. Schematic representation of the *P. patens* life cycle.
Gametophytic (nuclear phase, 1n) development starts with the germination of spores and the outgrowth of the filamentous protonema tissue. Bud formation gives rise to the adult moss plant (gametophore), which carries the sex organs (antheridia and archegonia). After fertilization of the egg cell, the diploid sporophyte develops (spore capsule). Adapted from Decker and Reski (2004).

Despite the long evolutionary distance between mosses and the flowering plants (*e.g.*, the model higher plant, *A. thaliana*), the latter of which has been the predominant subject of plant biology especially at the gene level, there are several reasons why this moss plant is suitable organism to use as a model system. Importantly, growth and propagation of *P. patens* is easily established and maintained on simple mineral media and under standard laboratory conditions, and it can readily regenerated from a single protoplast and almost any tissue of *P. patens* is

capable of regeneration (Cove, 1992). It has a short and relatively simple life cycle, as mentioned above. The entire genome of *P. patens* has been sequenced (Rensing *et al*., 2007). Furthermore, it is unique among model plants in that it has the capacity for efficient homologous recombination, enabling efficient gene targeting for functional analysis of genes (Schaefer and Zrÿd, 1997). Therefore, this moss is an attractive model plant in various fields of plant research, in particular from an evolutionary point of view.

Very recently, two independent groups (including the one that I belong to) recently compiled and investigated clock components in *P. patens* which would be orthologs of the circadian clock components in *A. thaliana* (Okada *et al*., 2009a; Holm *et al*., 2010). Interestingly, though homologs to a majority of the *A. thaliana* clock component genes were identified in all flowering plants so far examined, some prominent homologs such as GI and ZTL are missing in *P. patens* (Table 1). Okada *et al*. (2009) isolated and characterized two *P. patens* cDNAs *PpCCA1a* and *PpCCA1b* encoding moss homologs of *A. thaliana* CCA1/LHY, which function, as mentioned above, as important component proteins in the *A. thaliana* circadian network. It was also found that these genes displayed rhythmic expression profiles at the level of transcription in the continuous dark. Moreover, disruption experiments on *PpCCA1a* and *PpCCA1b* genes indicate that these two genes are functional counterparts of *CCA1/LHY* (Okada *et al*., 2009). These data suggest that a subset of the components in the circadian clock in higher plants were present at the emergence of land plants. To study the evolution of the circadian clock of land plants in more detail, it is important to characterize more clock component genes, such as *PRRs*, from *P. patens*.

Table 1. Comparative overview of clock components in *A. thaliana* and putative homologs in *P. patens* (NA: Not available or absent).

Arabidopsis thaliana				***Physcomitrella patens***		
Gene	**Locus ID**	**Protein features**	**Reference**	**Gene / gene model**	**Locus ID/tag**	**Reference**
LHY *CCA1*	At1g01060 At2g46830	Single Myb domain	Schaffer *et al*., 1998, Wang and Tobin 1998	*PpCCA1a* *PpCCA1b*	AB458831.1 AB458832.1	Rensing *et al*., 2008; Okada *et al.* 2009.
TOC1/ PRR1	At5g61380	Pseudo-response regulator, CCT	Strayer *et al.* 2000	NA	-	
PRR9 *PRR7* *PRR5* *PRR3*	At2g46790 At5g24470 At5g02810 At5g60100	Pseudo-response regulator, CCT	Makino *et al.*, *2000*	*PpPRR1* *PpPRR2* *PpPRR3* *PpPRR4*	AB558266 AB558268 AB558267 AB558269	Rensing *et al*., 2008; Satbhai *et al*., 2010 (In press).
LUX (*PCL1*)	At3g46640	Single Myb (GARP) domain	Hazen *et al.*, 2005; Onai and Ishiura 2005.	*PpLUX1-3*	Phypa_47310	Holm *et al*., 2010; Aoki *et al.* (unpublished)
ELF4	At2g40080	DUF1313	Kikis *et al.*, 2005	*PpELF4*	Phypa_49622	Holm *et al*., 2010; Aoki *et al.* (unpublished)
ELF3	At2g25930	Unknown	Hicks et al., *1996*	*PpELF3-1* *PpELF3-2*	Phypa_66647 Phypa_165364	Holm *et al*., 2010; Aoki *et al.* (unpublished)
CKB3 *CKB4*	At3g60250 At2g44680	CKII beta regulatory subunit	Sugano *et al.*, 1998	*PpCKB3* 1-4	Phypa_219176 Phypa_59578 Phypa_116155 Phypa_75590	Holm *et al*., 2010; Aoki *et al.* (unpublished)
ZTL	AT5G57360	FKF1 like	Somers *et al.*, 2000	NA	-	
GI	At1g22770	Unknown	Park *et al*., 1999	NA	-	

1.5 Objectives of this work

In the work presented here, the first detailed analysis of PRR homologs in a plant outside of flowering plants is conducted, *i.e.*, in the moss *P. patens*. First, comparative sequence analyses were carried out to find any conservation or divergence of characteristic domains and motifs. Also, a phylogenetic analysis of the PRR sequences was carried out in order to investigate any possible evolutional linkages among related genes in green plants. *In-vitro* phosphotransfer assay was carried out in order to confirm whether or not the *P. patens* PRR proteins preserve RR property. As diurnal or circadian regulation of transcription appears to be a conserved feature among *PRR* genes of flowering plants, it is analyzed to what extent this regulation is conserved in the *P. patens PRR* genes. Moreover, to gain first insights into the functional conservation of *PRRs*, heterologous expression and characterization of a *P. patens* PRR protein was carried out in *A. thaliana* plant. Finally, I will discuss scenarios of the evolution and divergence of *PRR* homolog genes in green plants.

2. MATERIALS AND METHODS

2.1. Materials

2.1.1. Chemicals, enzymes, oligonucleotides and cloning vectors

Chemicals used for this work were purchased from Wako, Sigma-Aldrich, Toyobo, Takara-Bio and Invitrogen. Enzymes were purchased from Fermentas, Takara-Bio, Toyobo, New England Biolabs (NEB) and Invitrogen. Oligonucleotides were synthesized at Invitrogen and Sigma. Cloning vectors used were pGEM-T easy (Promega) and pENTR ™/D-TOPO® (Invitrogen).

2.1.2. Buffers, solutions and media

Standard buffers, solutions and media for biochemical and molecular biological methods were prepared as described (Sambrook *et al.*, 1989). Growth medium compositions for *P. patens* are as follows.

Stock solutions:

Stock B (x 100)

$MgSO_4$ $7H_2O$	25 g (0.1 mM)
	Fill up to 1000 ml with H_2O, and autoclave

Stock C (x 100)

KH_2PO_4	25 g (1.84 mM)
	Adjust to pH6.5 with 4M KOH
	Fill up to 1000 ml with H_2O, and autoclave

Stock D (x 100)

KNO_3	101 g (1 M)
$FeSO_4$ $7H_2O$	1.25 g (4.5 mM)

	Fill up to 1000 ml with H_2O

Alternative TES (x 1000) Autoclave

$CuSO_4$ $5H_2O$	55 mg (0.22 mM)
H_3BO_3	614 mg (10 mM)
$CoCl_2$ $6H_2O$	55 mg (0.23 mM)
$Na2MoO_4$ $2H_2O$	25 mg (0.1 mM)
$ZnSO_4$ $7H_2O$	55 mg (0.19 mM)
$MnCl_2$ $4H_2O$	389 mg (2 mM)
KI	28 mg (0.17 mM)
	Fill up to 1000 ml with H_2O, and autoclave

500mM Ammonium Tartrate (x 100)

Ammonium Tartrate	92.05 g
	Fill up to 1000 ml with H_2O, and autoclave

50mM $CaCl_2$ (x 50)

$CaCl_2$ $2H_2O$	7.35 g
	Fill up to 1000 ml with H_2O, and autoclave

Media:

BCD+1mM Ca medium (BCD)

H_2O	900 ml
Stock B	10 ml
Stock C	10 ml
Stock D	10 ml
Alternative TES	1 ml
50mM $CaCl_2$ $2H_2O$	20 ml (1 mM)
Agar (Sigma, A6924)	8 g (0.8%)
	Fill up to 1000 ml with H_2O, and autoclave

BCDAT medium

H_2O	900 ml
Stock B	10 ml
Stock C	10 ml
Stock D	10 ml
Alternative TES	1 ml
500mM Ammounim tartrate	10 ml (= 5 mM)
50mM $CaCl_2$ $2H_2O$	20 ml (= 1 mM)
Agar (Sigma, A6924)	8 g (= 0.8%)
	Fill up to 1000 ml with H_2O

BCDATG medium

BCDATG medium is BCDAT medium that is supplemented with 5 g/l glucose.

2.1.3. Bacterial strains

The following bacterial strains are used as hosts for the molecular cloning and transformation of *A. thaliana*. *Escherichia coli* DH5α, *E. coli* DB3.1, *E. coli* BL21, *E. coli* DAC903 and *Agrobacterium tumefaciens* EHA 101 (only EHA 101 is for transformation of *A. thaliana*).

2.1.4. Plant materials

The following plants were used for experiments. *Physcomitrella patens* ssp. *patens* (Ashton and Cove, 1977), *A. thaliana* Columbia ecotype (Col-0), *A. thaliana CCA1::LUC* (Col-0) (Nakamichi *et al*., 2004), *A. thaliana* 35S::PpPRR2 (Col-0) and *A. thaliana* 35S::PpPRR2 (*CCA1:: LUC*/Col-0). The generation of the last two strains is described in 2.2.11.2.

2.1.5. Sequences on the databases

The sequences of the four *P. patens PRRs* have been submitted to and will appear in due course in the public databases (DDBJ/EMBL/GenBank): PpPRR1 (AB558266), PpPRR2 (AB558268), PpPRR3 (AB558267), PpPRR4 (AB558269). Accession numbers of other protein sequences used for phylogenetic analyses and alighments are as follows: SmPRR7a (450934, protein ID in the JGI *Selaginella moellendorffii* database), SmPRR7b (450936), SmTOC1 (438647) from *S. moellendorffii*; OtTOC1 (BAD38854 in DDBJ/EMBL/GenBank) from *Ostreococcus tauri*, AtPRR3 (BAB13744), AtPRR5 (BAB13743), AtPRR7 (BAB13742) and AtPRR9 (BAB13741) from *Arabidopsis thaliana*. OsTOC1 (BAD38854 in DDBJ/EMBL/GenBank), OsPRR37 (BAD38855), OsPRR73 (BAD38856), OsPRR59 (AK120059) and OsPRR95 (BAD38857) from *Oryza sativa*; PtTOC1 (XP_002330130.1 in NCBI protein database), PtPRR37 (XP_002311123.1), PtPRR73 (XP_002316333.1), PtPRR5a (XP_002321349.1) , PtPRR5b (XP_002301442.1), PtPRR9a (XP_002320232.1) and PtPRR9b (XP_002301443.1) from *Populus tricocharpa*; VvTOC1 (XP_002281757.1), VvPRR37 (XP_002281776), VvPRR73 (XP_002275645), VvPRR5 (XP_002270811), and VvPRR9 (XP_002266192.1) from *Vitis vinifera*; CrPRR1 (XP_001695777.1), CrPRR2 (XP_001701808.1) from *Chlamydomonas reinhardtii*; CvPRR1 (EFN58892.1 in Genbank) from *Chlorella variabilis*; LjTOC1 (chr4.CM0087.600.nc in miyakogusa.jp; http://www.kazusa.or.jp/lotus/index.html), LjPRR3 (LjT08O17.180/130/120), LjPRR5 (chr1.CM0105.560), LjPRR7 (chr3.LjT05P05.60) and LjPRR9 (chr3.CM0208.230) from *Lotus japonicus*.

2.1.6. Oligonucleotides

Table 2 A) Primers used for cloning of the four *PRR* cDNA sequences are summarized.

Primer name	Gene	Sequence (5' to 3')	Function
PRR1-5'Fw1	PpPRR1	CAG AAG CCC AAC TCC GGA CAG ACG	Gene Racing
PRR1-5' Fw2	PpPRR1	TTC GCG TCT TCC AGC AGC CCC CAG	Gene Racing
PRR1-Mid-Fw	PpPRR1	CTG CGG TTG CGA ATG GGT CGA TTG	Gene cloning

PRR1-Mid-Rv	PpPRR1	CTC CTT TCT CTT CTG CCT GAA CTT G	Gene cloning
PRR1-3'Fw1	PpPRR1	CGA ACG CCA ACA GCG GGA ATA ATG GA	Gene Racing
PRR1-3' Fw2	PpPRR1	AGG AGC GGT GCT TTG AGA AGA AGG TG	Gene Racing
PRR1RT-Fw	PpPRR1	AGA GCT TGT GGA GGA GGA GCA GGT GGA	Full length cDNA
PRR1RT-Rv	PpPRR1	CAT CCT CCA AAA TGA ACA CCA TCC TAC	Full length cDNA
PRR2-5'Fw1	PpPRR2	CTC TCT TGC AAG CCT CCC GTT TCA A	Gene Racing
PRR2-5' Fw2	PpPRR2	CCG GAC AGA CAT GGC ATC ACC ACA	Gene Racing
PRR2-Mid-Fw	PpPRR2	GTG ATG CCA TGT CTG TCC GGA GTC	Gene cloning
PRR2-Mid-Rv	PpPRR2	GAA TTT GTT TAA GGC AGC CTC TCG	Gene cloning
PRR2-3'Fw1	PpPRR2	CAT GGA TGG GGT GAG TGG GGG CAA	Gene Racing
PRR2-3' Fw2	PpPRR2	TGC ACA GAG CAA ATG CGT TTC GCC	Gene Racing
PRR2RT-Fw	PpPRR2	TTC TTC GAA TCG CAA CTC ATA GCT CAC	Full length cDNA
PRR2RT-Rv	PpPRR2	CCC ATC ATA GAG AGA ATC CAC TGC GAA	Full length cDNA
PRR3RT-Fw	PpPRR3	CCG TGT AAC CAA ACA GCA GGT GTA G	Full length cDNA
PRR3RT-Rv	PpPRR3	CGC ATT CGC ATT CCT AAG CCC TGT C	Full length cDNA
PRR4-5'Fw1	PpPRR4	GGC TTA CAC TAC AAC GAC GAG AAA A	Gene Racing
PRR4-5' Fw2	PpPRR4	AAC GAC GAG AAA ACC TAC AGA AGC A	Gene Racing
PRR4-Mid-Fw	PpPRR4	GAC GGA CGT AGT GAT GCC ATA TCT G	Gene cloning
PRR4-Mid-Rv	PpPRR4	GCT CCT TTC TCT TCT GCC TAA ACT TA	Gene cloning
PRR4-3'Fw1	PpPRR4	AGA GTG GAT TTG GTG CGA CGC CGA	Gene Racing
PRR4-3' Fw2	PpPRR4	CAA TGC GTT TCG CCA GAC GAG AG	Gene Racing
PRR4RT-Fw	PpPRR4	CGT GCT TCT GTA GGT TTT CTC GTC GT	Full length cDNA
PRR4RT-Rv	PpCRR4	ATA TCC TAT TCG GCG TCA CCA GCA	Full length cDNA

Table 2 B) Primers used in Sq-RT-PCR analyses are summarized.

Primer name	Gene	Sequence (5' to 3')	Optimal cycle number/Function
PRR1-Fw	PpPRR1	GGT GGA GTA TGA CGA CGC AAC AAG G	16
PRR1-Rv		TCC GTC ATC GTT CTC ACT CCC TTC A	
PRR2-Fw	PpPRR2	TAA GCA GGT GCG GGA GAA GTA GAG	16
PRR2-Rv		GAC TCC GGA CAG ACA TGG CAT CAC	
PRR3-Fw	PpPRR3	TCC GGT TTT ATG CTG GAG TTG AGT	20
PRR3-Rv		GTG GTG GTG ATG GTG GTG GTG ATG	
PRR4-Fw	PpPRR4	AGC CAC AGA CCC AGG ATG CAG AAC	16
PRR4-Rv		TGG TGG TGG TGC ATG TGC TGG TGA	
PpActin3U1	Actin	CGG AGA GGA AGT ACA GTG TGT GGA	16
PpActin3D1		ACC AGC CGT TAG AAT TGA GCC CAG	

AtAct8-Fw	Actin	GTC GCT GTC GAC TAC GAG CAA G	Control gene
AtAct8-Rv		CTG TGG ACA ATG CCT GGA CCT GC	

Table 2 C) Primers used for protein expression experiments are summarized.

Primer name	Gene	Sequence (5' to 3')	Function
PRR1-RLD-F	PpPRR1	ac GGT ACC GTT GGC TGG GAA AGC TTC C ct TCT AGA AGT CTG GCT GCC ACT CCC G	Protein expression
PRR1-RLD-R			
PRR2-RLD-F	PpPRR2	cc GGT ACC GGT GAC AGT TGG GAA AGC ct TCT AGA AGT CTG ATT GCC ACT TCC	Protein expression
PRR2-RLD-R			

*Kpn*I and *Xba*I restriction sites are underlined in forward and reverse primer, respectively.

Table 2 D) Primers used for the functional (overexpression) study are summarized.

Primer name	Gene	Sequence (5' to 3')	Function
PRR2-35sFw	PpPRR2	CAC CAT GAC TGC AGA TTT GAG CGA GGT TGA	Overexpression
PRR2-35sRv		TCC ACT GCG AAG ACG AAA AAA C	Overexpression

2.2. Methods

2.2.1. Plant growth conditions and light treatment

Physcomitrella patens ssp. *patens* (Ashton and Cove, 1977) and its derivative transformant strain were maintained in 12-hour light 12-hour dark cycles (12:12LD) under white fluorescent light (light intensity is approximately 40 μmol m^{-2} sec^{-1}) at 25°C. Protonemal and gametophore tissues were grown on BCDAT/G medium and BCD medium, respectively, both supplemented with 1 mM $CaCl_2$ (Nishiyama *et al*., 2000). Protonemal cells were collected every 5 to 7 days, and were ground with a homogenizer before application to new BCDAT agar plates. For light sources of the light induction experiments, the light-emitting diodes (STICK LED, Tokyo Rikakikai) were used for blue light (λmax = 470 nm) and the red-emitting fluorescent tubes (FL20S-Re-66, Toshiba Lighting & Technology) filtered through a red plastic sheet

(Acrylite102, Mitsubishi Rayon) for red light (λmax = 660 nm). White light was provided by fluorescence lumps (FL20SS-W/18, Toshiba Lighting & Technology).

A. thaliana (Columbia accession (Col)) were mainly used as wild-type plants. *A. thaliana* plants (Col) expressing the *CCA1::LUC+* reporter was constructed previously (Nakamichi *et al*. 2004). Seeds were imbibed and cold treated at 4°C for 3 days in the dark before germination under light, and then plants were grown at 22°C. Note that the imbibed seeds were exposed to white light for 30 min before incubation in the dark. Plants were grown in a chamber with light from fluorescent lights (70–80 μmol m^{-2} s^{-1}) at 22°C on soil and/or agar plates containing MS (Murashige and Skoog) salts and 1% sucrose. Transformant lines of *A. thaliana* that overexpress *PpPRR2* were maintained with the same conditions except that they were grown on the agar plates that contain bialaphos sodium salt (20 μg/ml) only when selecting resistant seedlings. 12:12LD and DD conditions were used for the bioluminescence assays.

2.2.2. Nucleic acid techniques

2.2.2.1. DNA and RNA isolation

Plasmid DNA was routinely isolated by boiling method (Sambrook *et al*., 1989) or by alkaline lysis method (Birnboim and Doly, 1979); large amounts were isolated using the Plasmid Midi/Maxi kit (Qiagen). Electrophoretic separation of DNA fragments was carried out according to standard procedures (Sambrook *et al*., 1989). *P. patens* total DNA was isolated as described (Physcobase, NIBB, Japan). Concentration of isolated DNA was determined by electrophoretic comparison with a λ-DNA standard, by agarose gel electrophoress or spot test (Sambrook *et al*., 1989). Plant total RNA was prepared by using RNAeasy Plant Mini kit (Qiagen) as per manufacturer's instructions. Concentration of isolated RNA was determined by standard spectrophotometric measurement (Sambrook *et al*., 1989).

2.2.2.2. Digestion and ligation

Digestion and ligation of DNA fragments with restriction enzymes and with ligases, respectively, were carried out according to the manufacturer's instructions and in the provided buffers.

2.2.2.3. Polymerase chain reaction (PCR) amplification

Standard PCR amplifications were carried out with Taq polymerase (Takara-Bio) or with KOD plus polymerase Ver.2 (Toyobo) using the standard PCR mixture composition and cycling profile (Sambrook *et al.*, 1989).

2.2.2.4. cDNA synthesis

cDNA was synthesized using Superscript II (Invitrogen) and random primers (Invitrogen) according to the manufacturer's instructions.

2.2.2.5. Nucleid acid sequencing

For plasmid DNAs, sequencing reactions were performed by using BigDye-terminator v3.1 cycle sequencing kit (Applied Biosystems). DNAs were sequenced by the Center for Gene Research (CGR, Nagoya University) sequencing service. On the other hand, PCR products were sequenced with DYEenamic ET terminator (GE Healthcare (Former Amersham Biosciences))

2.2.3. Sequence analysis

Standard sequence analysis was performed using the DNASIS software (Hitachi software engineering). Database searches were routinely carried out using the BLAST algorithm (Altschul *et al.*, 1997) at GenBank/DDBJ/NCBI (http://www.ncbi.nlm.nih.gov). For the identification of *PRR* genes from *P. patens*, database searches were performed using TBLASTN (Altschul *et al.*,

1997) with the PRR protein sequences as query sequences at JGI genome database (http://genome.jgi-psf.org/Phypa1_1/Phypa1_1.home.html) or at Physcobase (Nishiyama *et al*., 2003; http://moss.nibb.ac.jp).

2.2.4. Identification and isolation of *PpPRR* cDNAs

The *PpPRR1*cDNA was obtained as previously described (Okada *et al*., 2009). The 5'- and 3'-terminal portions of the *PpPRR2* and *PpPRR4* cDNAs were RACE-amplified using GeneRacer (Invitrogen) with primers based on the JGI database sequences. The amplified cDNA fragments were cloned into the pGEM-T Easy vector (Promega) and sequenced with DYEenamic ET terminator (GE Healthcare (Former Amersham Biosciences). The middle region of each gene was amplified by RT-PCR with primers based on the RACE-amplified sequences. The entire regions of both cDNAs were amplified with KOD plus polymerase Ver.2 (Toyobo) subjected to A-tailing by *Taq* polymerase (Takara-Bio) cloned into the pGEM-T Easy vector and sequenced using a primer walking method. The entire region of the *PpPRR3* cDNA was amplified with KOD plus polymerase Ver.2 using primers directly based on the JGI database sequences. Nucleotide sequences were assembled by DNASIS software (Hitachi software engineering). All primer sets used are described in Table 2A.

2.2.5. Phylogenetic analyses

Amino acid sequences deduced from cDNA sequences of *PRR* homologs were aligned using the ClustalW program (Higgins & Sharp, 1988) and the numbers of amino acid substitutions between each pair of PRR proteins were estimated by the Jones–Taylor–Thornton (JTT) model (Jones et al., 1992) with the complete-deletion option. From estimated numbers of amino acid substitutions, a phylogenetic tree was reconstructed using the Molecular Evolution

(ME) method (Rzhetsky & Nei, 1992). The bootstrap values were calculated with 1000 replications (Felsenstein, 1985). These procedures were all performed using MEGA4.1 software (http://www.megasoftware.net/index.html; Tamura et al., 2007). We also reconstructed a phylogenetic tree by using RLD sequences by using bacterial RR as the out-group by similar method .We obtained similar phylogeny pattern in both trees.

2.2.6. Semi-quantitative reverse-transcription (RT)-PCR analysis and quantitative real-time (RT)-PCR analysis

Total RNA (1 μg) was reverse-transcribed by using a cDNA synthesis kit (Takara-Bio) with oligo (dT-16) primer, and 1/18.6 of the reaction mixture was subjected to semi-quantitative reverse-transcription PCR (sqRT-PCR) analysis. Preliminary experiments were conducted to improve its quantitativeness as follows. First, thermal cycle numbers were optimized so that signals from PCR products did not reach a plateau. Next, I confirmed that, when various known relative amounts of cDNA for each tested gene were used as PCR templates, the amount of the PCR product of each reaction showed a linear relationship with that of the input cDNA. The primers and optimal cycle numbers for PCR are described in Table 2B. Primer sets for *PRR* genes are based on sequences of both sides of the intron of each *PRR* gene so that genomic amplification could be distinguished (Hara *et al*. 2001). The resulting PCR products were fractionated on an agarose gel, Southern blotted onto the nylon membrane (Hybond-N+, Amersham Biosciences) and probed with cDNA for each target sequence. The cDNA probes were amplified using the primer sets above described and were labeled by using DIG DNA labeling and detection kit (Roche Diagnostics). The digitized signals of the *PRR* products were normalized by the signals of the *actin* PCR products. Probe preparation and blotting procedures were carried out as per manufacturer's instructions. Quantitative real-time PCR (qRT-PCR) analysis was performed as previously described (Nakamichi *et al*., 2007). The primers are same as those used in the sqRT-PCR analysis.

2.2.7. Construction of vectors for expression of PpPRR1 and PpPRR2 receiver-like domain (RLD) peptides

To express the PpPRR1 and PpPRR2 RLD peptides in *E. coli* cells, a cold shock expression system (pCold-II vector; Takara-Bio) was used as follows. The coding region for the RLD of each PpPRR protein was PCR-amplified with primers described in Table 2C. The resultant fragment was cloned into the pGEM-T Easy vector, digested with *Kpn*I and *Xba*I, and inserted into *Kpn*I-*Xba*I-cleaved pCold-II vector (pCold-II-His-PRR1 and pCold-II-His-PRR2 for PpPRR1 RLD and PpPRR2 RLD, respectively). The nucleotide sequence was determined by DYEenamic ET terminator. The RLD peptides are fused with a 6xHis-tag, by expression from pCold-II vector, allowing their purification with a TALON metal affinity resin column as described below.

2.2.8. Expression and purification of the PpPRR1 and PpPRR2 RLD peptides

The *E. coli* strain BL21 (DE3) harboring pG-KJE8 (Takara-Bio), which encodes chaperone proteins DnaK, DnaJ, GrpE, GroEL and GroES, was transformed with pCold-II-His-PRR1 or pCold-II-His-PRR2. To overproduce the RLD peptides of PpPRR1 and PpPRR2, each transformant was cultivated in 1 L of LB medium containing ampicillin (50 μg/ml), chloramphenicol (25 μg/ml), tetracycline (20 ng/ml) and L-arabinose (10 mg/ml) at 37°C until the logarithmic phase of growth in a rotary shaker (at 110 rpm). They were cold-shocked by standing at 15°C for 30 minutes after the addition of IPTG at the final concentration of 1 mM and cultured in a shaker (at 110 rpm) at 15°C for 5 hours. Cells were collected by centrifugation and suspended in 20 ml of a standard buffer (50mM Tris-HCl [pH 8.0], 100mM NaCl and 10% glycerol). The cell suspension was mixed with DNase I (25 μg/ml), EDTA (1.25 mM), and lysozyme (250 μg/ml) at 4°C for 15 min, and then passed through a French Press at 100 MPa. The resultant cell lysate was centrifuged and separated from cell debris and then applied onto a

TALON^{TM} metal affinity resin (Clontech Laboratories) column. After washing the TALON column with 50 mM Tris-HCl (pH 8.0), 10% glycerol, and 100 mM NaCl, each of 6xHis-tagged PpPRR1 and PpPRR2 RLD peptides was eluted with the same buffer including 250 mM imidazole and finally dialyzed against 50 mM Tris-HCl (pH 8.0) and 10% glycerol. Dialyzed semi-purified protein was concentrated by loading on Amicon Ultra Filter (Ultracel-10K; Millipore) and centrifuged for 15 min at 4700 rpm at 4 °C. The sample was quantified by the Lowry method (Lowry *et al*., 1951) and subjected to SDS-PAGE and detected with Coomassie Brilliant Blue. It was also analyzed by Western blotting with anti-6xHis antibodies (Cat. No. A190-114A; Bethyl Laboratories).

2.2.9. Preparation of the *E. coli* ArcB–enriched cytoplasmic membrane

E. coli DAC903/pIA001-ArcB and DAC903/pIN-III were used as an ArcB overproducer and a negative control, respectively (Tsuzuki *et al*., 1995). From each strain, membrane vesicles were isolated and pelleted as an insoluble fraction of the cell lysate according to the method of Azuma *et al*. (2007). They were suspended in a small volume of a buffer comprising 50 mM Tris-acetate (pH8.0), 1 mM DTT, 2% glycerol and 250 mM sucrose in order to isolate cytoplasmic membrane as follows. The suspended membrane vesicles were layered over a 21 ml 5 steps-gradient of sucrose dissolved in the same buffer (3 ml of 50%, 9 ml of 45%, 3 ml of 40%, 3 ml of 35% and 3 ml of 30% from bottom to top) in a bottle assembly polycarbonate tube (part no. 355618; Beckman Coulter) and centrifuged at 47,000 rpm for 2 hours at 4˚C with the type 50.2 Ti rotor (Beckman Coulter). The cytoplasmic membrane was collected by taking the fraction between the layers of 35% and 40% sucrose and diluted with a large volume of a buffer (T_AGS-buffer) comprising 50 mM Tris-acetate (pH 7.8), 1 mM DTT, 10% glycerol, 100 mM sucrose. The cytoplasmic membrane was collected by centrifugation at 127,000 X *g* for 2 h and then resuspended in a small volume of T_AGS-buffer. Finally F_1-ATPase was stripped from the cytoplasmic membrane as follows. The isolated cytoplasmic membrane (2 mg of protein) was treated with 1 ml of T_AGS-buffer containing 4 M urea for 30 min on ice, and then recovered by centrifugation at 50,000 rpm for 30 min. Then the pellet was washed once

with 1 ml of TGS-buffer and finally with 1 ml of a buffer comprising 50 mM Tris-HCl (pH 8.0), 2 mM DTT and 10% glycerol. The urea-treated cytoplasmic membrane was suspended in 0.5 ml of the same buffer and stored at -80 ˚C.

2.2.10. *In vitro* autophosphorylation assay

In vitro autophosphorylation reaction of the ArcB protein was carried out according to the method of Azuma *et al*. (2007). 4.0 μg of ArcB-enriched *E.coli* cytoplasmic membrane was incubated with 0.05 mM γ-[^{32}P]-ATP (37 kBq) in TEG buffer (50 mM Tris HCl pH 8.0, 0.35 mM EDTA, 10% glycerol) containing 5 mM $MgCl_2$, 200 mM KCl and 2 mM DTT at 25°C for 1, 5 and 10 min. 4.0 μg of *E. coli* cytoplasmic membrane which was prepared from the strain which does not overproduce ArcB was also used as a negative control experiment. The reaction was terminated by the addition of SDS-PAGE sample buffer (finally 20 mM Tris-HCl (pH 8.0), 1% β-mercaptoethanol, 1% SDS, 6% glycerol and 0.02% bromophenol blue). The samples were subjected to SDS-PAGE. The gel was dried and analyzed with an imaging scanner (BAS-2500; Fuji Film).

2.2.11 *In vitro* His-Asp phosphotransfer assay

In vitro His-Asp phosphotransfer reaction from ArcB to the RLD peptides of PpPRR1 and PpPRR2 was examined according to the method of Azuma *et al*. (2007). 4.0 μg of *E.coli* ArcB-enriched cytoplasmic membrane was incubated with 0.05 mM γ-[^{32}P]-ATP (37 kBq) and 4.5 μg of semi-purified PpPRR1 or PpPRR2 RLD peptide in TEG buffer (50mM Tris HCl pH 8.0, 0.35 mM EDTA, 10% Glycerol) containing 5 mM $MgCl_2$, 200 mM KCl and 2 mM DTT at 25°C for 1, 5 and 10 min. The reaction was terminated by the addition of SDS-PAGE sample

buffer. The samples were subjected to SDS-PAGE. The gel was dried and analyzed with BAS-2500.

2.2.12. Constructs for *A. thaliana* transformation

The transforming constructs were generated by using Gateway cloning technology (Invitrogen). The coding sequence of PpPRR2 was amplified by PCR using KOD plus polymerase Ver.2 with primers 5'-CACCATGACTGCAGATTTGAGCGAGGTTGA-3' / 5'-TCCACTGCGAAGACGAAAAAAC-3'from cDNA. They were integrated into the pENTR/D/TOPO entry vector, and then transferred to the pTK35S-GW-HA (destination vector) with LR clonase II (Invitogen) as per manufacturer's instructions.

2.2.13. Transformation and selection procedures

2.2.13.1. Bacterial transformation and selection

Electrocompetent *E.coli* cells were either purchased from Toyobo, or prepared according to the $CaCl_2$-method (Sambrook *et al*., 1989). Electrocompetent *A. tumefaciens* were prepared according to $CaCl_2$ (Sambrook *et al*., 1989) and stored at -80°C. Transformation and selection procedures were as described (Sambrook *et al*., 1989).

2.2.13.2. *A. thaliana* transformation and selection

The plasmid pTK35S-PpPRR2 was transformed into *A. tumefaciens* strain EHA101. A single colony resistant to 50 mg/l kanamycin and 50 mg/l spectinomycin was inoculated for pre-culture in liquid LB medium (Sambrook *et al*., 1989) supplemented with the same antibiotics at the same concentrations. The presence of the pTK35S-PpPRR2 plasmid in pre-culture was confirmed by PCR amplification using Taq polymerase (Takara-Bio) from a 1 µl culture aliquot

with the primers specific to *PpPRR2*. Then, the resulting construct was transformed into appropriate *A. thaliana* plants by vacuum infiltration procedures (Bechtold and Pelletier 1998). Transgenic lines segregating bialphos resistance as a single locus were used in further analyses.

2.2.14. Preparation of *A. thaliana* RNA and reverse transcription

RNA was purified with RNeasy Plant Mini Kit (Qiagen). cDNA was generated from 1.5 µg of each RNA sample digested by RNase-free DNase I (Qiagen) with ReverTra Ace (Toyobo) and oligo(dT) primer.

2.2.15. Flowering time analysis of *A. thaliana* transformants

Mutant seeds were sown on MS media with 1% agar and incubated in the dark for 48 hours at 4°C. Cold-treated seeds were then grown under long-day (15:9LD) or short-day (9:15LD) conditions at 22 °C. After 1 week seedlings were transfer on soil. Flowering time of each plant was evaluated quantitatively by counting the number of leaves when the primary inflorescence was detected.

2.2.16. Measurement of the hypocotyls length

For hypocotyls length measurements, seeds were sown on MS media with 1% agar and incubated in the dark for 48 hours at 4°C. Cold-treated seeds were then grown under long-day (15:9LD) or short-day (9:15LD) conditions at 22°C. Hypocotyl lengths of seedlings were measured by using a digital camera (Kodak DCS 420) and the IMAGE program (National Institutes of Health).

2.2.17. Examination of light response in early photomorphogenesis

To avoid any influence of carbohydrates and growth media components on photomorphogenesis (Fankhauser and Casal, 2004, Virtudes *et al*. 2007), *A. thaliana* seeds were sown on four layers of filter paper and allowed to imbibe in sterile water in the dark for 48 hours at 4 °C. Then, seeds were exposed to white light for 6 hours in order to enhance germination, followed by incubation at 22°C for 18 hours again in the dark. Plants were grown for 72 hours under continuous light with an appropriate fluence rates or in the dark. As the light sources for continuous irradiation, light-emitting diodes (LEDs) were used: for red light, STICK-mR (λmax = 660 nm at 4 μmol m^{-2} $sec^{-1}$and 40 μmol m^{-2} sec^{-1} (Tokyorika).

2.2.18. Monitoring and data analysis of bioluminescence from the *A. thaliana* luciferase reporter lines

The plasmid pTK35S-PpPRR2 was used to transform the *A. thaliana* plants expressing the *CCA1::LUC+* reporter (Nakamichi *et al*., 2004). Transformation was performed as described in 2.2.11.2.section. Independent transgenic (T1) lines were obtained by selecting resistant seedlings on MS plates containing bialaphos sodium salt (20 μg/ml) in 10 days after germination. They were used for bioluminescence assays as follows. The resistant plants selected were transferred on MS plates which contained luciferin (5 μM) and grown for 3 days in 12:12LD under white fluorescent light (70 μmol m^{-2} s^{-1}) for entrainment. The plates containing young seedlings were then subjected to bioluminescence measurement by the real-time bioluminescence monitoring system as described previously (Kondo *et al*., 1993, Nakamichi *et al*., 2004). During the measurement of luciferase activity, plants were released from 12:12LD to DD conditions. Rhythm data were analyzed using the Biological Rhythm Analysis Software System (BRASS, Southern *et al*., 2007), available at http://millar.bio.ed.ac.uk/PEBrown/BRASS/BrassPage.htm, with fast Fourier-transform non-linear least-squares estimation.

3. RESULTS

3.1. Identification, Isolation and characterization of *PRR* homolog genes in *P. patens*.

Based on extensive search in the JGI *P. patens* genome database, I found four gene models that are significantly similar to the *A. thaliana PRR* genes: *PpPRR1* (protein ID in the JGI database: 154145), *PpPRR2* (165025), *PpPRR3* (173125) and *PpPRR4* (165029). Next, I isolated cDNAs that cover the entire coding regions for the *PpPRR1*, *PpPRR2*, *PpPRR3* and *PpPRR4* genes. The coding DNA sequences of four *PpPRRs* were aligned to each other and to the genomic sequences (from JGI database) to determine the exon-intron structure and the transcript boundaries (Fig. 6).

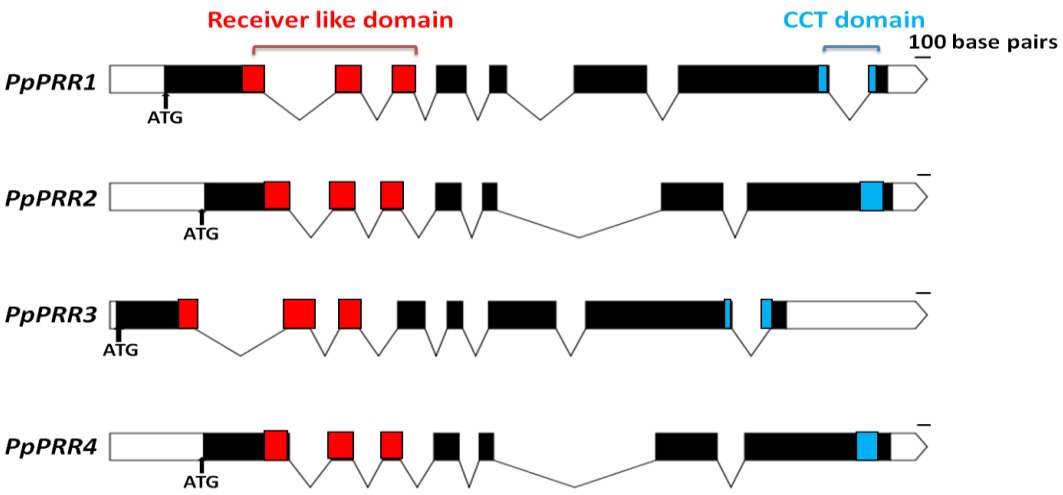

Figure 6. Schematic representation of the genomic sequences of *PpPRR1, PpPRR2, PpPRR3* and *PpPRR4*. Exons and introns are indicated by filled boxes and lines, respectively. The untranslated regions in exons are indicated by open boxes. Two conserved domains specific to *PRR* genes are shown by red color (RLD at amino-terminus) and blue color (CCT domain at carboxy-terminus). Scale bar above each gene represents a 100-bp sequence.

The nucleotide sequences of the coding regions of the four genes are well related to each other: 79% (identify for PpPRR1/PpPRR2), 96% (PpPRR1/PpPRR3), 79% (PpPRR1/PpPRR4), 79% (PpPRR2/PpPRR3), 84% (PpPRR2/PpPRR4) and 79% (PpPRR3/PpPRR4). Thus, the sequence alignment of coding regions clearly showed that PpPRR1/PpPRR3 and PpPRR2/PpPRR4 shared more significant homologies than other combinations. The stretches of amino acids with clear sequence diversity between PpPRR1/3 and PpPRR2/4 are shown in Fig. 7 by red rectangular boxes. All of their predicted proteins share, as do *AtPRRs*, an amino-terminal RLD and a carboxy-terminal CCT domain. Domain sequences are shown by red color lines (RLD) and blue color lines (CCT domain) above the sequences (Fig. 7).

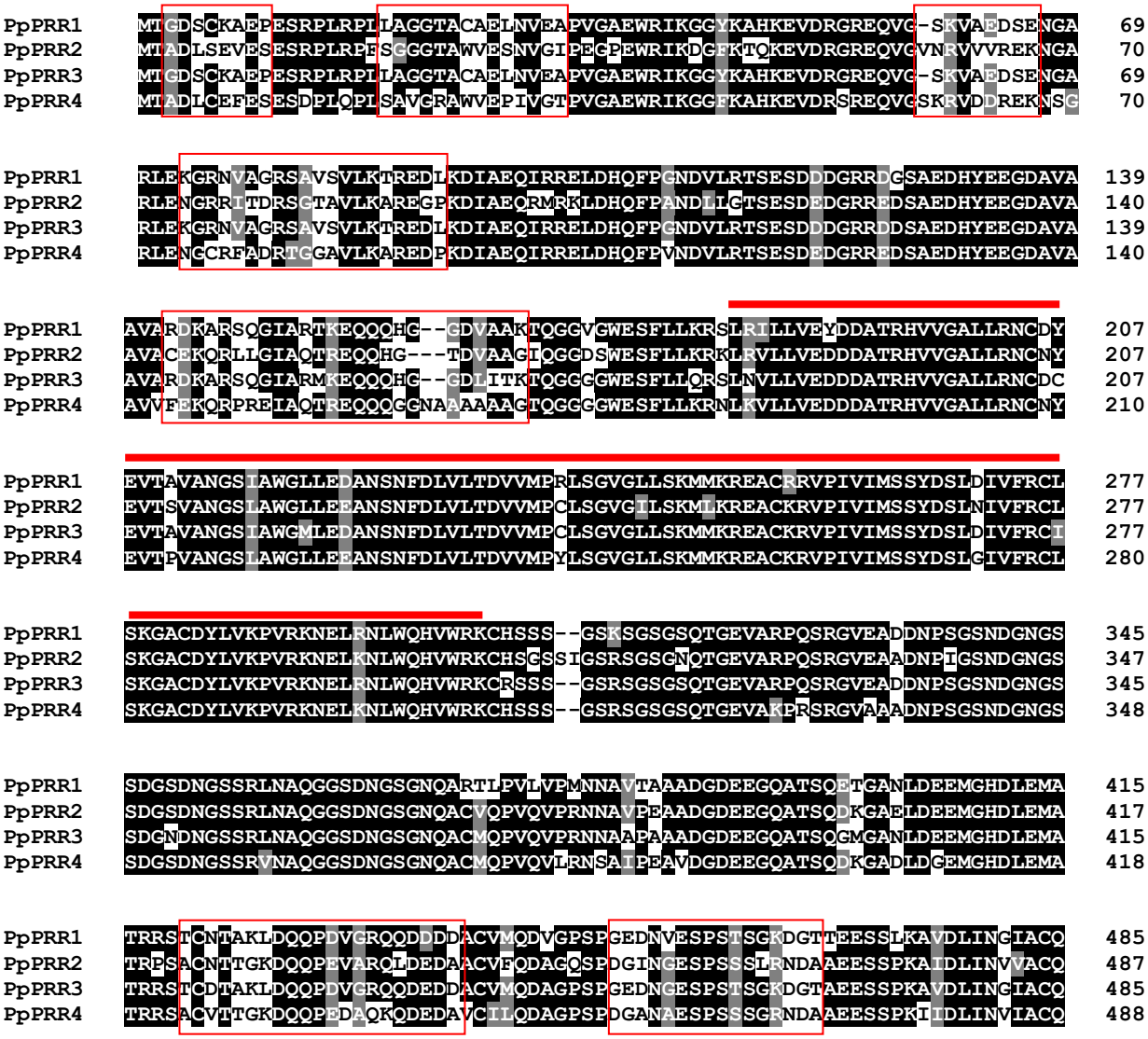

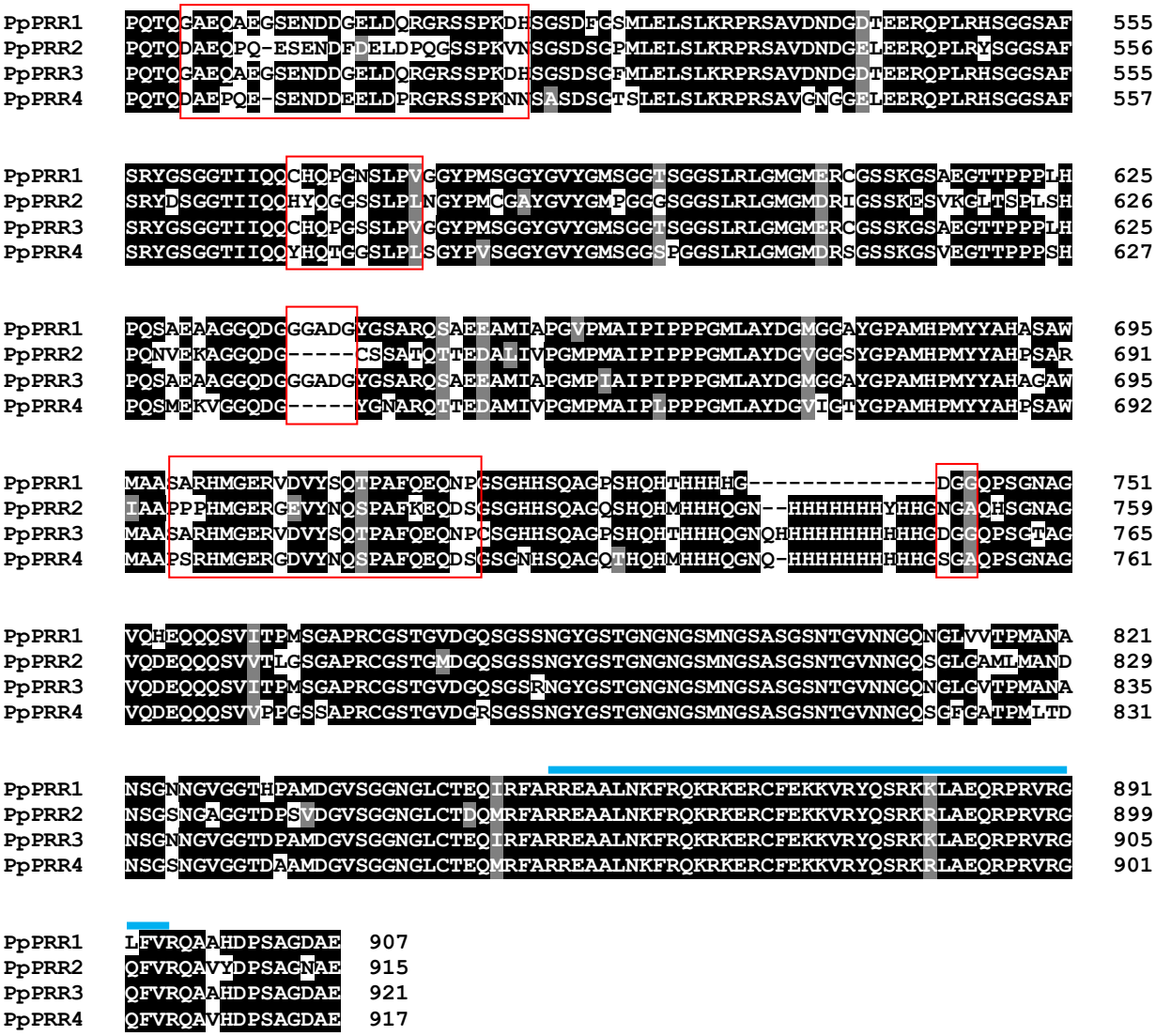

Figure 7. Amino acid sequence alignment of PpPRRs. Complete coding region sequences of PpPRR1, PpPRR2, PpPRR3, and PpPRR4 are aligned using ClustalW program (Higgins & Sharp, 1988). Shading was performed using BOXSHADE ver 3.21 (http://www.ch.embnet.org/software/BOX_form.html). Amino acids identical or similar in more than 70% of the sequences are shaded by black or grey background, respectively. The number at the end of each line indicates the rightmost amino acid. Two conserved domains specific to PRR genes are shown by red color (RLD at amino-terminal) and blue color (CCT domain at carboxy-terminal) lines above the sequence. Red rectangular boxes represent the sequence stretches diverged between PpPRR1/3 and PpPRR2/4.

The receiver domains of authentic RRs share the aspartic acid-aspartic acid-lysine (DDK) motif, essential for the phosphotransfer activity (Parkinson and Kofoid, 1992; Ueguchi *et al.*, 2001), whereas the first two residues of this motif are diverged in the flowering plant PRR proteins (Fig. 8a; for review, see Mizuno and Nakamichi, 2005 and Mizuno, 2005). In all the available flowering plants PRR sequences, the second aspartic acid, conserved as the phosphoacceptor residue in the His-Asp phosphotransfer, is replaced by a glutamic acid (E) (Fig.8a, Fig.8c). In contrast, RLDs of moss PpPRR proteins are all predicted to retain the second aspartic acid; furthermore, PpPRR2, PpPRR3 and PpPRR4 also retain the first aspartic acid, hence exhibiting the complete DDK motif (Fig.8a, Fig.8c). PpPRR1 replaces the first aspartic acid residue with a tyrosine (Y) (Fig.8 a, Fig.8c). These observations suggest that at least PpPRR2, PpPRR3 and PpPRR4 are potentially phosphorylated by a HK(s) as authentic RRs. The CCT domain is well conserved in all PpPRR proteins (Fig. 8b).

(a)

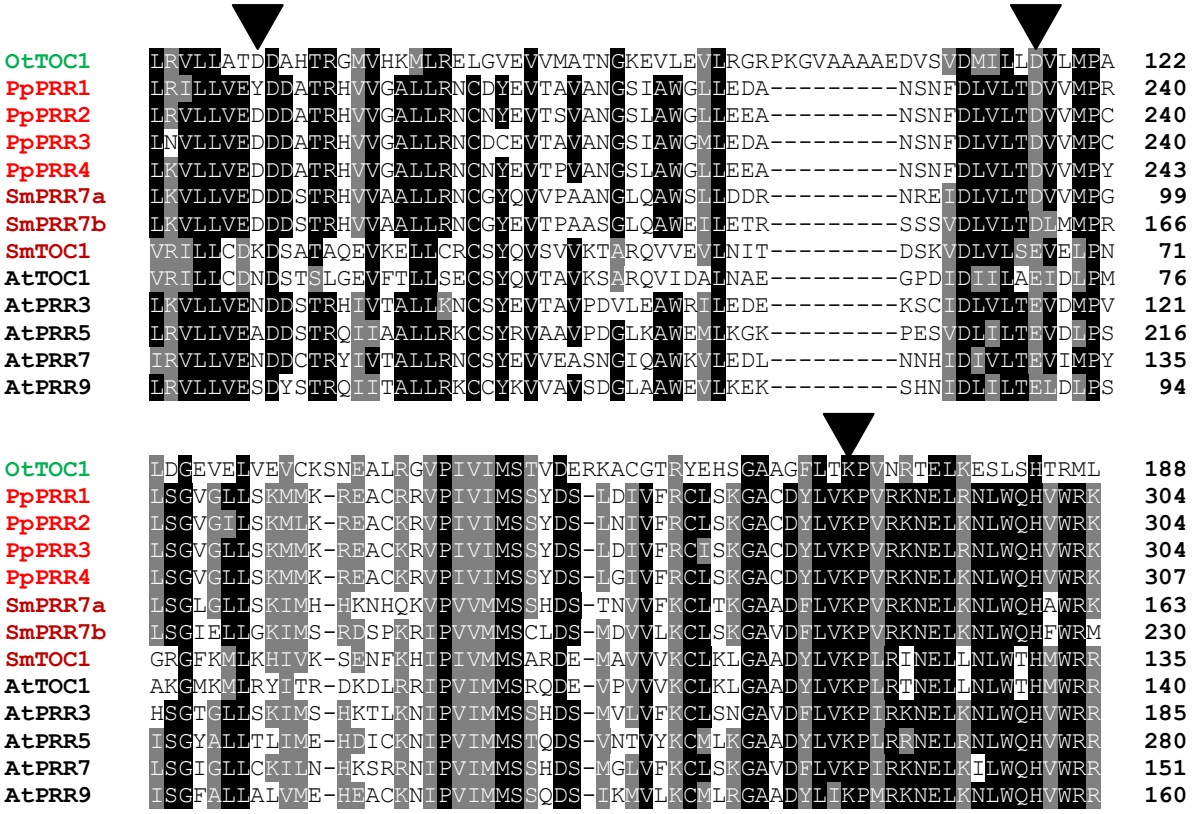

(b)

```
OtTOC1      HRAAAIRRFLKKRKERNFDKKVRYASRQQLAASRPRLRGQFVR  514
PpPRR1      RREAALNKFRQKRKERCFEKKVRYQSRKKLAEQRPRVRGLFVR  895
PpPRR2      RREAALNKFRQKRKERCFEKKVRYQSRKRLAEQRPRVRGQFVR  903
PpPRR3      RREAALNKFRQKRKERCFEKKVRYQSRKKLAEQRPRVRGQFVR  909
PpPRR4      RREAALNKFRQKRKERCFEKKVRYQSRKRLAEQRPRVRGQFVR  905
SmPRR7a     RREAALNKFRQKRKERCFEKKVRYQSRKRLAEQRPRVRGQFVS  633
SmPRR7b     RREVALYKFRQKRKERCFEKKVRYQSRKRLAEQRPRIKTKIND  817
SmTOC1      RREAALHKFRQKRKDRCYEKKIRYASRKRLAEQRPRVKGQFVR  476
AtTOC1      RREEALLKFRRKRNQRCFDKKIRYVNRKRLAERRPRVKGQFVR  574
AtPRR3      QREAALMKFRLKRKERCFEKKVRYHSRKKLAEQRPHVKGQFIR  483
AtPRR5      QREAALTKFRMKRKDRCYEKKVRYESRKKLAEQRPRIKGQFVR  659
AtPRR7      QREAALTKFRQKRKERCFRKKVRYQSRKKLAEQRPRVRGQFVR  710
AtPRR9      QREAALMKFRLKRKDRCFDKKVRYQSRKKLAEQRPRVKGQFVR  458
```

(c)

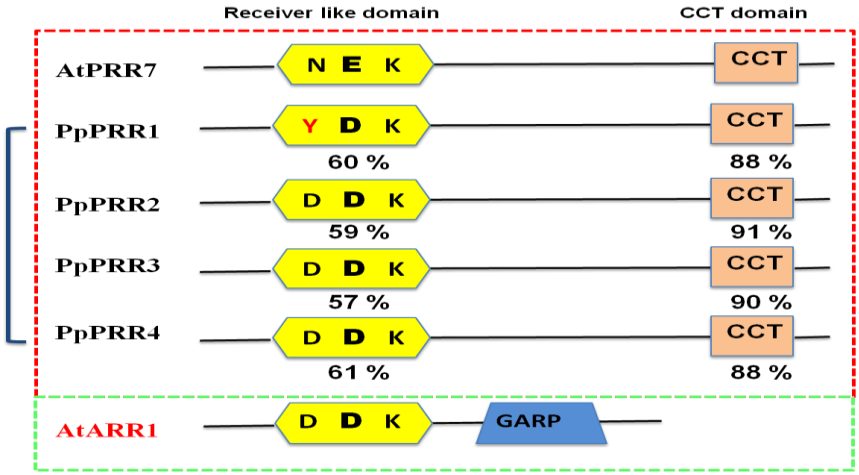

Figure 8. Alignment of conserved domains of PRR homologs from various species. RLDs (a) and CCT domains (b) of PRR homolog sequences from various plant species are aligned as described in legend of Fig. 7. Arrowheads show amino acids corresponding to the DDK motif. The PRR homolog sequences are as follows: PpPRR1, PpPRR2, PpPRR3 and PpPRR4 from *P. patens*; SmPRR7a, SmPRR7b, and SmTOC1 from *Selaginella moellendorffii* from *S. moellendorffii*; OtTOC1 from *Ostreococcus tauri*; AtTOC1/PRR1, AtPRR3, AtPRR5, AtPRR7 and AtPRR9 from *A. thaliana*. (c) Comparison of domain structures of PpPRRs with AtPRR7 and AtARR1 from *A. thaliana*. Sequence identify to the corresponding region of AtPRR7 is shown below each domain.

To examine evolutionary relationships among *PpPRRs* and other land plant *PRRs*, I constructed a phylogenetic tree using PRR homolog sequences from various plants (Fig. 9). The *PRR* homolog of the green alga *O. tauri* (*OtTOC1*, see Corellou *et al*., 2009), was used as outgroup because OtTOC1 is positioned relatively distant from any other PRR homolog sequences (Holm *et al*., 2010). I confirmed that, when an authentic RR sequence is used as the outgroup, OtTOC1 is placed outside of all the other PRR homolog sequences (Fig. 10). Also included were three algal sequences: two from *Chlamydomonas reinhardtii* and one from *Chlorella variabilis*. In the phylogenetic tree, the angiosperm sequences are divided, as previously reported (Murakami *et al*., 2003; Miwa *et al*., 2005; Takata *et al*., 2010), into three groups: TOC1, PRR7/3 and PRR9/5 (Fig. 9). The TOC1 group is basal to all the other sequences that include both PRR7/3 and PRR9/5 groups, indicating a more ancient origin of the TOC1 group than the other two groups. The four moss PpPRR sequences are grouped with one another, further forming a cluster with two lycophyte sequences, and this cluster is sister to the PRR7/3 group (Fig. 9). This indicates that the moss *PpPRR* genes are more closely related to the PRR7/3 group than to the two other groups. The four moss sequences are divided into two groups PpPRR1/PpPRR3 and PpPRR2/PpPRR4 (Fig. 9). The distinction between *PpPRR1/PpPRR3* and *PpPRR2/PpPRR4* genes is also reflected in sequence alignment as shown in Fig. 7 (Red squares).

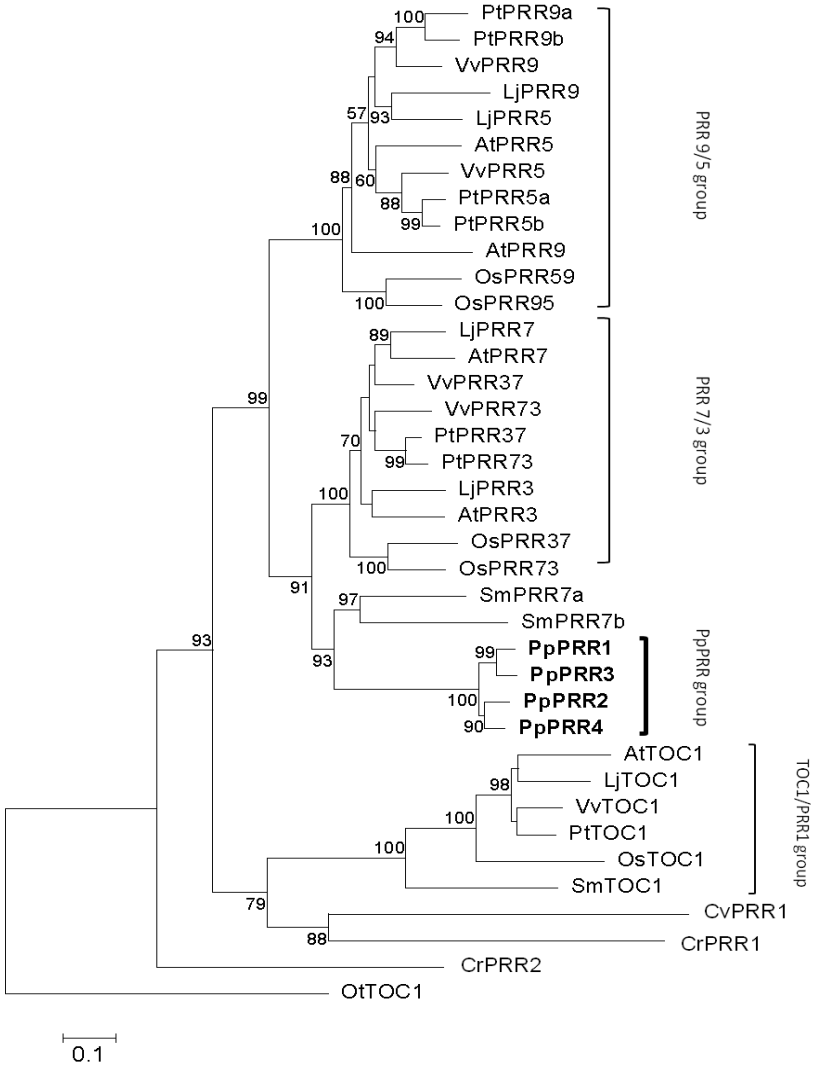

Figure 9. Phylogenetic tree of PRR homologs in various plants. Amino acid sequences of PRR homologs including entire RLD and CCT domain regions were aligned using ClustalW program and the phylogenetic tree was reconstructed by the Minimum Evolution (ME) method by using MEGA4.1. The *Ostreococcus tauri* PRR homolog (OtTOC1) was used as the outgroup. The numbers at each node represent bootstrap values calculated based on 1000 bootstrap sampling and those that are higher than 50% are shown. PpPRRs from *P. patens* are indicated in bold. Accession numbers of sequences used are given in Materials and Methods section.

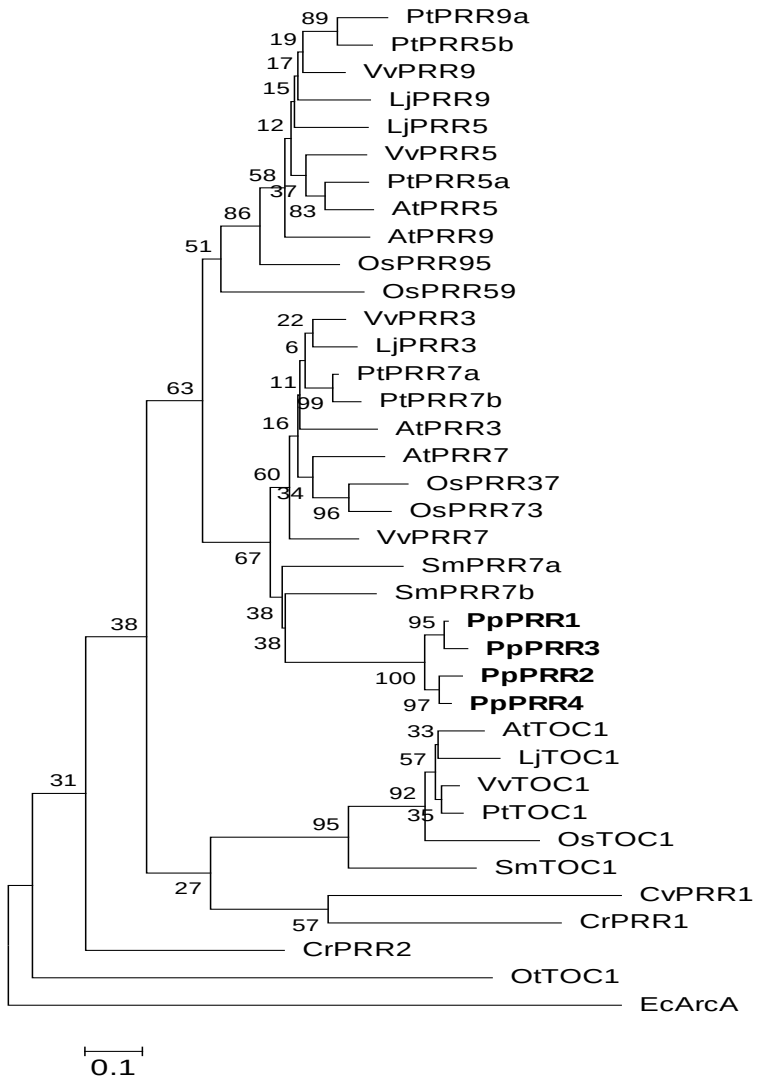

Figure 10. Phylogenetic tree of PRR homologs in various plants by using RLD domain sequences and an *E. coli* RR sequence as the outgroup. Amino acid sequences of PRR homologs including entire RLD regions were aligned using ClustalW program and the phylogenetic tree was reconstructed as described in Fig. 9 legend. The *E.coli* (EcArcA) sequence used as the outgroup. The numbers at each node represent bootstrap values calculated based on 1000 bootstrap sampling and those that are higher than 50% are shown. PpPRRs from *P. patens* are indicated in bold.

Next, comparisons of the distribution of intron insertion sites on the RLD and CCT coding regions between *PRR* genes was carried out (Fig. 11). In the RLD region, two insertion

sites are conserved among all the *PRR* sequences examined (Figs. 1a and 11; see Takata *et al*., 2010). This distribution pattern of intron insertion sites is clearly different from those seen in the receiver domain of authentic RRs (Ishida *et al*., 2009), confirming the idea that *PRR* genes diverged distinctly from authentic *RR* genes. In the CCT domain region, the TOC1 group sequences are unique in that they show no intron whereas all sequences in the other two groups have a conserved single insertion site in the middle of the domain (Fig. 11; see Takata *et al*., 2010). *PpPRR* sequences are divided into two groups, *PpPRR1/PpPRR3* with one intron (like the PRR7/3 and PRR9/5 groups) and *PpPRR2/PpPRR4* with no intron (like the TOC1 group) (Fig. 11). This divergence is consistent with the results of the phylogenetic tree (Fig. 9), whereas the loss of an intron in *PpPRR2/PpPRR4* should have occurred in the moss lineage independently from the TOC1 group (Fig. 9).

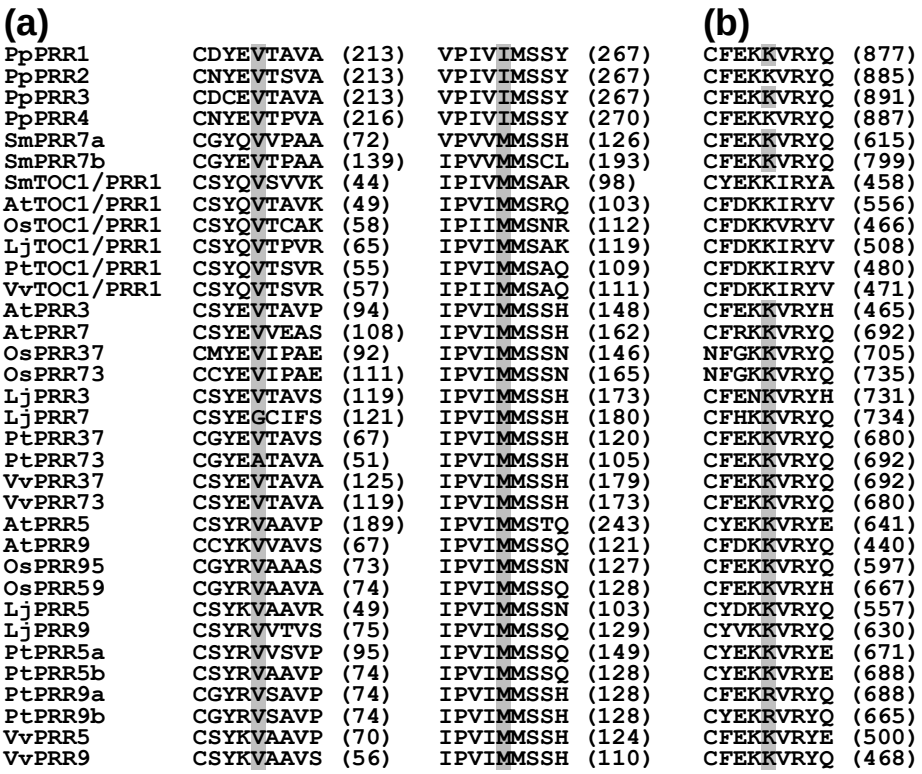

Figure 11. Distribution of intron insertion sites on the conserved domains of PRR sequences. From the aligned amino acid sequences of PRR proteins, only three stretches (two from RLD (a) and one from CCT (b)) are shown, each consisting of nine amino acids with the amino acid corresponding to an intron insertion site (shaded in grey) being centered. The number of the rightmost amino acid of each stretch is indicated in parentheses.

3.2. *In-vitro* phosphotransfer assay of PpPRR proteins

As mentioned in the above section, all higher plants studied before do not have phosphotransfer ability as their RLD domain sequences are diverged from authentic RRs. This study is the first report demonstrating that the early land plant *P. patens* PRR sequences retain the RR type features (complete D-D-K motif is retained in PpPRR2, PpPRR3 and PpPRR4 and the phosphoaccpetor aspartic acid (D) residue in PpPRR1 (Fig. 8). Next, I studied whether RLDs of PpPRR1 and PpPRR2, both of which retain the potential phosphoacceptor residue while showing mutually diverged features (Fig. 8c), are phosphorylated by a His-Asp phosphorelay process in an *in-vitro* phosphotransfer assay (Fig. 12). In this assay, ArcB, an *Escherichia coli* HK, added in excess and hence lacking substrate specificity, transfers its phosphate to the phosphoacceptor site in a receiver domain. I have purified the RLD peptides of PpPRR1 and PpPRR2 overexpressed in *E. coli* cells (Fig. 12b and 12c, respectively) and tested each of them to assess whether or not they undergo phosphotransfer. The PpPRR2 RLD peptide was phosphorylated within 5 minutes in the presence of ArcB (Fig. 12g). The phosphorylation levels of ArcB decreased concomitantly (Fig. 12g), indicating that the phosphorylation of PpPRR2 RLD is due to phosphotransfer from ArcB. On the other hand, no phosphorylation signal was detected with PpPRR1 RLD (Fig. 12f), consistent with its relatively diverged RLD sequence (Figs. 8a and 8c). When the PpPRR2 RLD peptide was incubated with the membrane fraction with no overexpressed ArcB, phosphorylation signal was not found (Fig. 12h). This supports the interpretation that the increased levels of phosphorylation seen with the PpPRR2 RLD peptide (Fig. 12g) is due to phosphotransfer from ArcB, but not due to other types of kinases. These observations indicate that PpPRR2 presumably functions as an RR in an unknown His-Asp phosphorelay signal transduction pathway in *P. patens*. Moreover, PpPRRs likely diverged from one another based not only on their RLD sequences but also on their phosphotransfer ability.

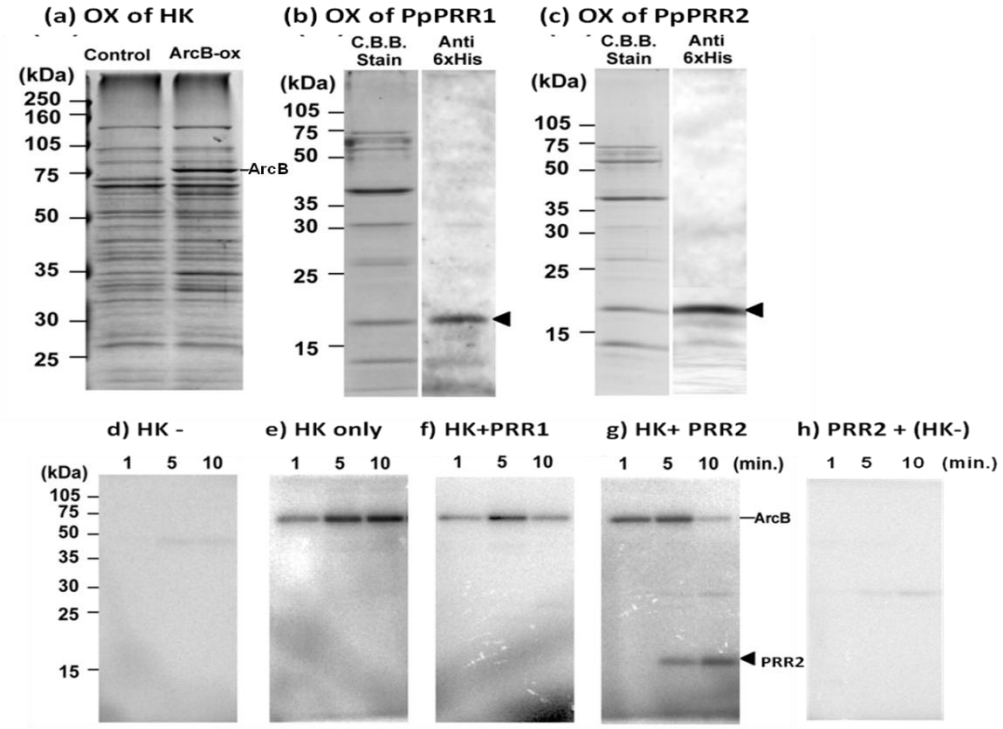

Figure 12. ***In vitro*** **His-Asp phosphotransfer to the PpPRR2 RLD peptide.**

(a) Overproduction of ArcB in *Escherichia coli* cells. The cytoplasmic membrane proteins were extracted from an ArcB overproducer (right lane) and a negative control strain of *E. coli* (left lane), subjected to SDS-PAGE and detected with Coomassie Brilliant Blue (C.B.B.) (see Materials and Methods for further details). The ArcB band of around 88 kDa is indicated. Purification of PpPRR1 (b) and PpPRR2 (c) RLD peptides is shown. PpPRR1 and PpPRR2 RLD peptides were respectively affinity-purified with TALON^{TM} metal affinity resin from soluble protein fraction of cell lysate of each overproducer strain, subjected to SDS-PAGE and detected with C.B.B. Existence of PpPRR1 and PpPRR2 RLD peptides were further confirmed by Western blotting with anti-6xHis antibodies; PpPRR1 and PpPRR2 RLD peptides (~17 kDa for each) are indicated with closed triangles. (d), (e) Results of autophosphorylation assay. *E. coli* ArcB-enriched membranes (e) or control membranes (d) were incubated with γ-[^{32}P]-ATP for indicated times. (f)-(h) Results of *in vitro* His-Asp phosphotransfer assay. *E. coli* ArcB-enriched membranes were incubated with γ-[^{32}P]-ATP for indicated times in the presence of PpPRR1 (f) or PpPRR2 (g) RLD peptide. A reference reaction was conducted using control membranes incubated with γ-[^{32}P]-ATP for indicated times in the presence of PpPRR2 RLD peptide (h). Signals from the gels were analyzed by BAS-2500 for their phosphorylation status.

3.3. Transcriptional regulation of *PpPRR* genes

3.3.1. Circadian regulation of *PpPRR* expression profiles

Circadian regulation of transcription is an essential feature of *PRR* genes that function in *A. thaliana*. Interestingly, rhythmic fluctuations in transcript abundance are conserved among *PRR* genes from flowering plants. Besides, most of clock-associated genes or their homologs from any other plant species that was analyzed to date showed diurnal or circadian fluctuations of transcript abundance. The *A. thaliana PRR* gene family consists of five members (*TOC1, PRR3, PRR5, PRR7, and PRR9*), all of which are regulated by the circadian clock, but each of which peaks at different times of the day: *PRR9* mRNA levels are greatest at dawn, *PRR7* peaks in the morning, *PRR5* around noon, and *PRR3* and *TOC1/PRR1* in the evening (Matsushika *et al*., 2000). The expression profile of the functional orthologs from rice is almost identical, to the expression profile of *AtPRR*s (Murakami *et al*., 2003). I examined whether or not this regulatory mechanism is also shared by *PRR* genes of *P. patens.*

In order to determine the expression patterns of *PpPRR1, PpPRR2, PpPRR3* and *PpPRR4*, mRNA abundance was analyzed in 12-hour light 12-hour dark cycles (12:12LD), in continuous darkness (DD), and in continuous light (LL) by semi-quantitative RT-PCR (sqRT-PCR; Fig.13). In 12:12LD, all genes showed high-amplitude mRNA rhythms with a period of approximately one day, which peaked in the latter half of the light phase (Fig. 13a). In DD, all genes showed endogenous rhythms with damping (Fig. 13b). These rhythms in 12:12LD or DD showed phase relationships roughly similar to *A. thaliana PRR3*, *PRR5* or *PRR7* genes (Mizuno, 2005a, 2005b). In LL, in contrast, all the genes exhibited no hint of circadian regulation and were arrhythmic as demonstrated for *PpPRR1* (Fig. 13c; Okada *et al*., 2009). The arrhythmic profiles in LL are consistent with our observations that the moss genes so far tested are, if clock gene homologs or clock-controlled genes, all arrhythmic in LL (Aoki *et al*., 2004; Ichikawa *et al*., 2004; Shimizu *et al*., 2004; Okada *et al*., 2009) and this is in contrast to flowering plants *PRR* genes, all of which show robust circadian rhythms in LL (Mizuno, 2005).

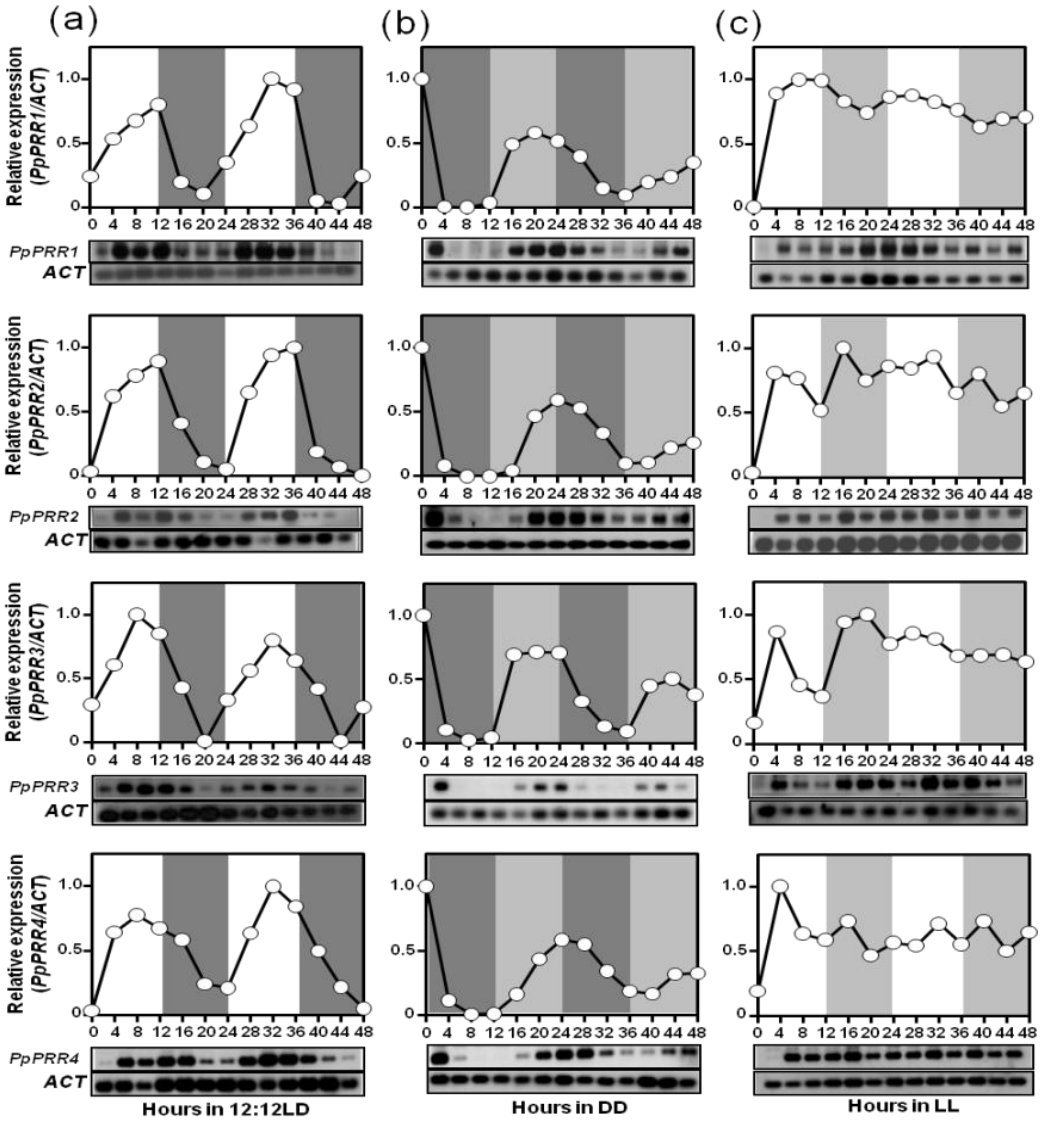

Figure 13. Changes in mRNA abundance for the *PpPRR* genes under 12:12LD, DD and LL conditions examined by the semi-quantitative RT-PCR analysis. *P. patens* protonemal cells were maintained in 12:12LD for more than two weeks after which cells were harvested in 12:12LD (a), DD (b) or LL (c) conditions at indicated times. From the top, changes in mRNA abundance for *PpPRR1*, *PpPRR2*, *PpPRR3* and *PpPRR4* are shown. Light conditions are overlaid with each graph: regions with no shade and those shaded with dark grey represent light and dark phases, respectively; regions shaded with light grey represent subjective light phases in (b) or subjective dark phases in (c). Graphs show the results of quantification of the mRNA levels for each gene after normalization to those for *actin* as control. The maximum levels are set

to 1.0. The photo below each graph shows the hybridized bands for each test gene or the control *actin* gene, detected as chemiluminescence signals. Similar results were obtained in two independent experiments.

The results of the sqRT-PCR experiments suggest that phases of the four genes seem to be differentially fine-tuned into two types: in 12:12LD, troughs of *PpPRR1/PpPRR3* occurred four hours before dawn, whereas those of *PpPRR2/PpPRR4* just at dawn (Fig. 13a). Additionally, I measured mRNA accumulation for *PpPRRs* in one cycle of 12:12LD by the quantitative real-time PCR (qRT-PCR) analysis with a shorter sampling interval (Fig. 14). At ZT01 (ZT, zeitgeber time: time in a light-dark cycle, putting the light onset as ZT0), the levels of *PpPRR1/PpPRR3* showed certain increase (30 to 40 % of the maximum levels) whereas those of *PpPRR2/PpPRR4* were still very close to zero (Fig. 14), confirming the distinction of expression profiles between *PpPRR1/PpPRR3* and *PpPRR2/PpPRR4*. This differential fine-tuning appears to be conferred by the endogenous circadian clock, because the sampling of cells at dawn (Fig. 14a, hours 0 and 24) was performed in the absence of light. This idea is also supported by the rhythms of *PpPRRs* in DD, where endogenous clock regulation is more clearly seen: the first peaks of *PpPRR2/PpPRR4* lagged behind those of *PpPRR1/PpPRR3* by around four hours (Fig. 14b; Fig. 15).

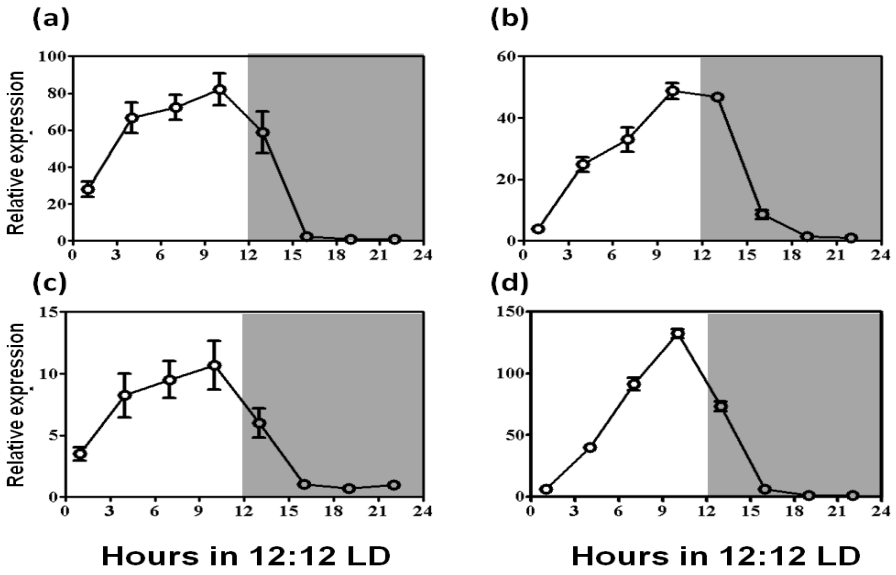

Figure 14. Changes in mRNA abundance for the *PpPRR* genes for one 12:12LD cycle examined by the quantitative real-time PCR analysis. *P. patens* protonemal cells were maintained in 12:12LD for more than two weeks after which cells were harvested in one full cycle of 12:12LD at indicated times. Shown are changes in mRNA abundance for *PpPRR1* (a), *PpPRR2* (b), *PpPRR3* (c), and *PpPRR4* (d). Light conditions are overlaid with each graph: regions with no shade and those shaded with dark grey represent light and dark phases, respectively. The graphs show the averages and standard deviations of four independent experiments, in which the results of quantification of mRNA levels for each gene were normalized to those of *actin* as control.

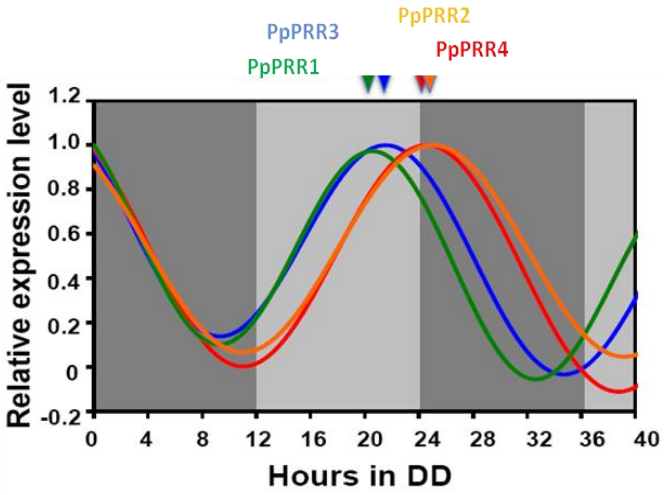

Figure 15. Comparison of phases for expression rhythms of the *PpPRR* genes in DD. The data used for Fig. 13b were analyzed with the Fast Fourier Transform-Nonliner Least Squares (FFT-NLLS) algorithm (Millar *et al*., 1995; Plautz *et al*., 1997) to quantitatively determine the phase positions of expression rhythms of *PpPRR* genes in DD. The resultant fitted curves and the first peak positions (21.55 h for *PpPRR1*, 20.98 h for Pp*PRR3*, 24.58 h for *PpRRR2* and 25.01 h for *PpPRR4*) for the four *PpPRR* genes are shown. The maximum expression level of each gene was set to 1.0 for clarity.

3.3.2. Induction of *PpPRR* by light

Several lines of evidence have already been reported to support the view that all *A. thaliana PRR* gene family members are important for better understanding of the molecular link between circadian rhythm and light-signal transduction (some references needed). Among the *AtPRR* family members, the *AtPRR9* gene is unique in that its expression is rapidly induced by light at the level of transcription (Ito *et al*., 2004). *AtPRR9* gene appears to play a crucial role in or close to the circadian clock and light-signal transduction pathways (Matsushika *et al*, 2002; Sato *et al*., 2002; Ito *et al*., 2003). I examined whether or not this regulatory mechanism in response to light is also shared by *PRR* genes of *P. patens*.

The effect of light on the accumulation of the *PpPRR* mRNAs was examined by sqRT-PCR analyses. The mRNAs of all four *PpPRRs* were induced by a 2-hour pulse of white, blue or red light (Fig. 16). The rates of induction by white light are 8.7 for *PpPRR1*, 2.6 for *PpPRR2*, 6.2 for *PpPRR3* and 2.5 for *PpPRR4*. The rates of induction for *PpPRR1* and *PpPRR3* are the highest and second highest, respectively, for any color of light; this observation does not contradict the idea that there is an intra-specific divergence between *PpPRR1/PpPRR3* and *PpPRR2/PpPRR4*. The rates of induction by blue light and red light are lower than those of white light for any *PpPRR* gene. The expression of each gene responded to white, blue and red light, suggesting responsiveness to integrated light signaling (Fig. 16).

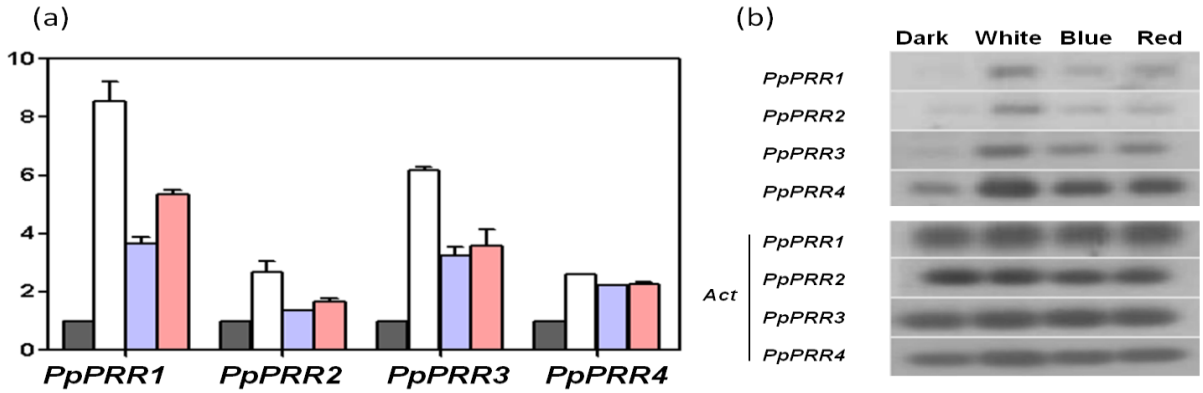

Figure 16. Light-induced expression of the *PpPRR* genes examined by the semi-quantitative RT-PCR analysis. *P. patens* protonemal cells were maintained under LL for one week, exposed to darkness for 24 hours, and 2 hours of white light, blue light, red light or dark period was

administered before the cells were sampled. The fluence rate of each light quality was 40 μmol m^{-2} s^{-1}. Total RNAs were extracted, and the abundances of *PpPRR* mRNAs were measured and normalized to those for *actin* as control. The graph shows the mRNA levels of *PpPRRs* induced by different qualities of light (the colour of each bar corresponds to that of light used for the measurement) relative to those from samples maintained in the prolonged darkness (dark grey bars), the latter of which are set to 1.0. Values are means ± SD of three replications. The bottom photos show the hybridized bands for *PpPRRs* (upper four slips) or the control *actin* gene for each *PpPRR* (lower four slips), detected as chemiluminescence signals. Similar results were obtained in two independent experiments.

3.3.3. *PpPRR* expression in *PpCCA1a/PpCCA1b* double disruptant strain

Above results consistently suggest that *PpPRR*s and *AtPRR*s shared significant similarities as well as some striking differences among them. In *A. thaliana*, as mentioned before, there are two negative feedback loops in which *CCA1/LHY* take part as one group: the *CCA1/LHY– TOC1*(*PRR1*) loop and the *CCA1/LHY–PRR5/PRR7/PRR9* loop (Mizuno and Nakamichi, 2005; Locke *et al*., 2006; McClung, 2006; Zeilinger *et al*., 2006). Subsequent work coupled *CCA1* and *LHY* as positive regulators of *PRR5, PRR7* and *PRR9* transcription, which act to negatively regulate *CCA1/LHY* (Farre *et al*, 2005). Previously, Okada *et al*., (2009) reported that *PpCCA1a* and *PpCCA1b* are functional homologs of *AtCCA1/LHY*. To see whether *PpPRRs* are controlled by the moss clock genes *PpCCA1a/PpCCA1b*, I compared their expression profiles between the wild type (WT) and the *PpCCA1a/PpCCA1b* double disruptant strain (Fig. 17). *PpCCA1a/PpCCA1b* double disruptant strain was generated as described previously (Okada *et al*., 2009).

Expression levels of each *PpPRR* were examined at the indicated time points during one cycle of 12:12LD (Fig. 17). The mRNA accumulation levels of all *PpPRR* genes increased significantly in the double disruptant strain compared to those in the WT strain, at around ZT03. These time-dependent increases are probably due to rhythmic expression of *PpCCA1a/PpCCA1b*. Since *PpCCA1a/PpCCA1b* peak at around dawn (Okada *et al*., 2009), the effects of derepression of *PpPRRs* are most prominent immediately after dawn.

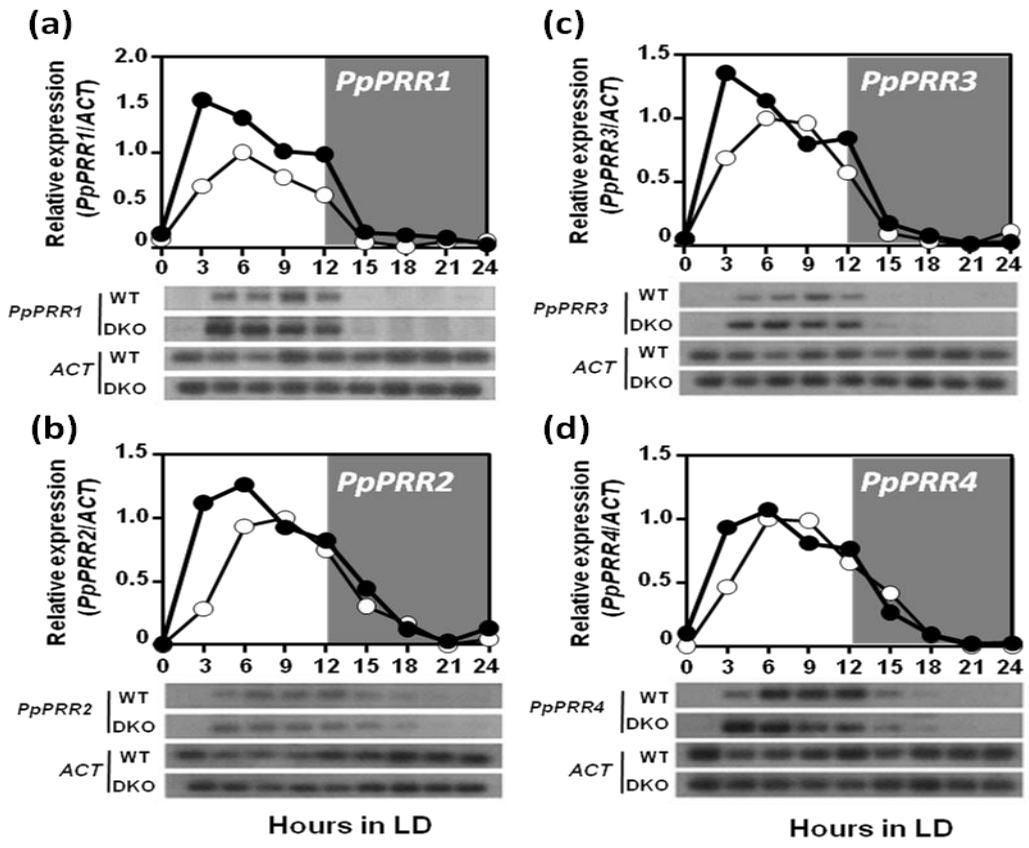

Figure 17. Changes in mRNA abundance for the *PpPRR* genes of the double disruptant. The *PpCCA1a*/*PpCCA1b* double disruptant strain used for this experiment was generated in a previous study (Okada *et al*., 2009). Measured are the mRNA accumulation levels of *PpPRR1* (a), *PpPRR2* (b), *PpPRR3* (c) and *PpPRR4* (d) in the WT strain (open circles) and the double disruptant (closed circles). The photos below the graph are representative results showing hybridized bands for each test gene or the control *actin* gene for the WT strain (WT) or for the double disruptant (KO). Experiments were performed as described in Figure 13.

3.4 Constitutive expression of the *PpPRR2* gene in *A. thaliana*

As shown in above sections *PpPRR*s and *AtPRR*s shared significant similarities (high sequence homology on conserved domains, circadian regulation, and light induced expression (see Fig. 8c, Fig. 13 and Fig. 16)) and differences (PpPRRs retained RR type features (D-D-K motif and phosphotransfer ability; Fig. 8c, Fig. 12)). Importantly, phylogenetic analysis clearly

showed that PpPRRs have close relationships to the higher plant PRRs (Fig. 9). Functions of *PRR* genes, therefore, appear to be at least partially shared with *PRRs* of flowering plants. It is widely accepted that *A. thaliana* plants with lesions or misexpression/ overexpression in clock-associated genes (*e.g.*, *PRR7* and *PRR9*) commonly display the following characteristic phenotypes with three biological events, (i) altered free-running expression profiles of circadian-associated genes, (ii) changes in photoperiodic dependent flowering time, and (iii) altered sensitivity toward red light during early photomorphogenesis (Farre *et al*., 2007; Matsushika *et al*., 2007). In this study, *A. thaliana* plants misexpressing *PpPRR2* (*PpPRR2*-OX) were characterized with reference to these clock-associated phenotypes. This work represents the first study of functional similarity of *PRR* genes in the early land plant *P. patens* and the flowering plant *A. thaliana.*

3.4.1 *PpPRR2* misexpression affects free-running rhythms of *AtCCA1*

For the research of circadian rhythms in plants, one of the most powerful and elegantly adopted techniques is the bioluminescence monitoring system for circadian gene expression. This system employs a transgenic plant carrying a transgene, in which a hallmarked circadian-controlled promoter is fused to the firefly luciferase gene (*LUC*), so as to easily monitor a given circadian profile *in planta* in real-time. *A. thaliana* wild type plants (Col) carrying the *CCA1::LUC* bioluminescence reporter is the convenient tool for real time monitoring of the circadian oscillation *in vivo* (Nakamichi *et al*., 2004).

The coding-sequence of *PpPRR2* was fused downstream of the CaMV 35S promoter as described in Methods section. T1 transgenic lines were selected on MS gellan gum plates containing appropriate antibiotics for 10 days. The resistant seedlings most likely harboring the 35S::*PpPRR2* transgene (*PpPRR2* misexpressing lines or *PpPRR2*-OX) were transferred onto MS gellan gum plates containing 5 µM firefly luciferin. They were grown for another 7 days to be entrained properly under 12:12LD cycles, and then released into DD to monitor the free-running rhythms of bioluminescence intensity, as described previously (Nakamichi *et al*., 2004). Wild type Col seedlings of the host reporter strain were also examined, as a reference. A representative result was shown in Fig. 18a. It was noticed that both the free-running rhythmic

profiles of the reference and the *PpPRR2* misexpressing line were robust in DD, but their profiles were not perfectly superimposed. The position of peak phase in the *PpPRR2* misexpressing line advanced gradually over time, compared with that of Col. The profile is indicative of the phenotype of short period. To further confirm the phenotype, the free-running profiles of wild type (n=11) and several independent T1 transgenic lines (n=11) were subjected to the fast Fourier transform non-linear least-squares analysis (FFT-NLLS, Millar *et al*., 1995), and relationship between the estimated period length and relative amplitude error in DD was shown in the graph (Fig. 18b). The result indicates clearly that free running rhythm of *CCA1*::*LUC* gene expression in *PpPRR2* misexpression lines is shorter than that in wild type under DD condition, suggesting that heterologous expression of *PpPRR2* modifies intrinsic property of the *A. thaliana* circadian clock.

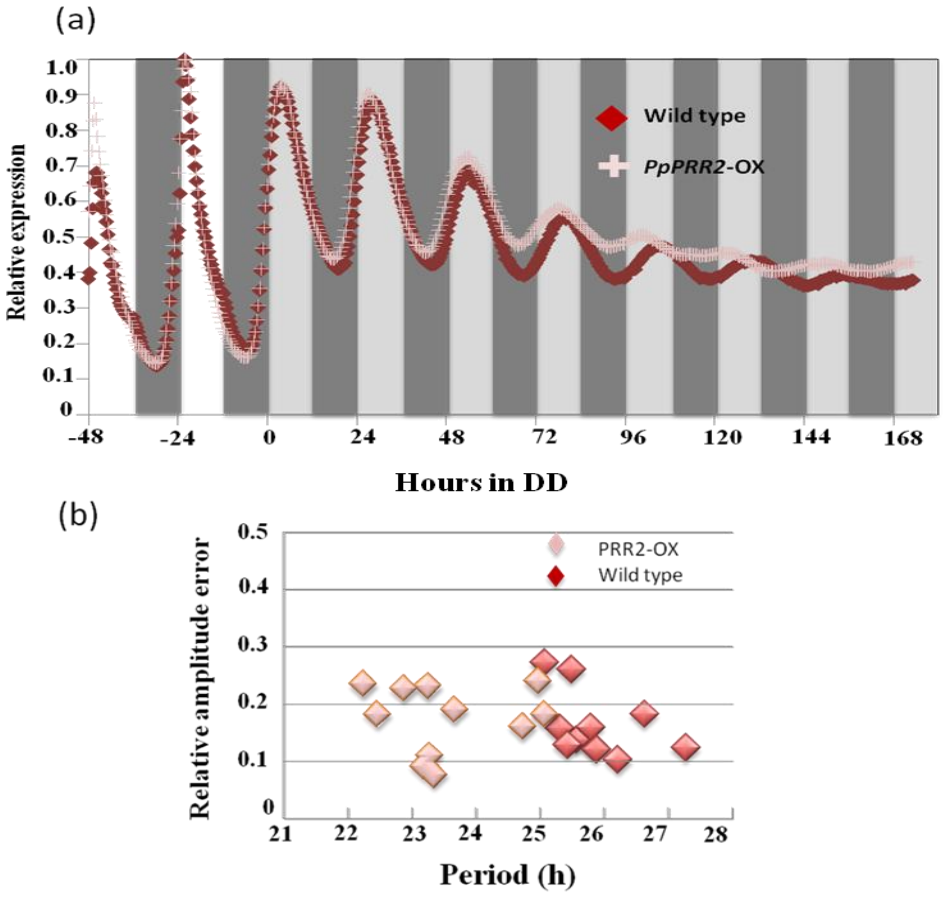

Figure 18. Modified intrinsic mechanism underlying the circadian clock caused by the heterologous expression of *PpPRR2* in *A. thaliana*. (a) A number of T1 transgenic lines

misexpressing *PpPRR2* were isolated using wild type Col plants carrying the *CCA1*::*LUC* reporter construct as a host. The control host strains (n=11) and the independent T1 transgenic lines (n=11) selected on MS-gellan gum plates containing 20 μM Bialaphos sodium salt were grown on MS-gellan gum plates containing 5 μM firefly luciferin for 7 days under 12:12LD, and then they were released into DD to monitor the free-running rhythms of bioluminescence intensity. The representative profiles were shown for Col (filled diamond) and Col-*PpPRR2*-OX (cross) respectively. (b) Period lengths and relative amplitude errors in the above experiment were estimated using fast Fourier transform non-linear least-squares analysis (FFT-NLLS).

3.4.2 Flowering time measurement in *PpPRR2* misexpressing plants

The most significant issue with regard to *PpPRR2* misexpressing plants, which should be addressed here, is whether or not they show any biological phenotype. To address this question, flowering time analysis is carried out. Several independent T2 transgenic seeds were isolated. After examining whether the segregation ratio of resistant to sensitive plants on the selection plates including bialaphos sodium salt was approximately 3:1, four independent transgenic lines (L3, L5, L7, and L9), which should harbor the monogenic 35S::*PpPRR2* transgene was established. Phenotypic characterization of these lines with reference to the photoperiodic control of flowering time was carried out. When seeds of the T2 transgenic plants were germinated and grown under long day conditions (15-hour light 9-hour dark cycles; 15:9LD), they set flowers as rapidly as in the case of Col (Fig 19a). When they were grown in short day conditions (9:15LD), however, some population of T2 plants set flowers earlier than did Col. The phenotype of early flowering was observed for all of the four independent lines tested (Fig. 19a). Therefore, a large number of T2 transgenic plants of a *PpPRR2* misexpressing line (L5) (n=114) were grown in short day, and their flowering time was evaluated quantitatively by counting the number of leaves when the primary inflorescence was detected (Fig. 19b). The result of Fig. 19b indicates that both the homozygous and heterozygous *PpPRR2* misexpressing lines exhibit the phenotype of early flowering, because statistically 75% of T2 populations showed the phenomenon, and remains showed the wild type property (see the legend to Fig.19b). To confirm this assumption, representatives of early and late flowering plants (five each) were selected (Fig. 19c). Then,

expression (or transcripts) of the *PpPRR2* transgene in these plants was examined with RT-PCR analyses. The results showed that the early flowering plants carried the *PpPRR2* transgene, but the late flowering plants did not (Fig. 19c). These results were consistent with the idea that when the *PpPRR2* gene was introduced into *A. thaliana* plants, the moss gene exhibited an ability to disturb the intrinsic regulatory pathway of the clock-mediated photoperiodic control of flowering time in the host. *AtPRR9* misexpressing plants (*AtPRR9*-OX), *AtPRR7*-OX and *AtPRR5*-OX plants also showed a similar phenotype of early flowering (Matsushika *et al*., 2002a).

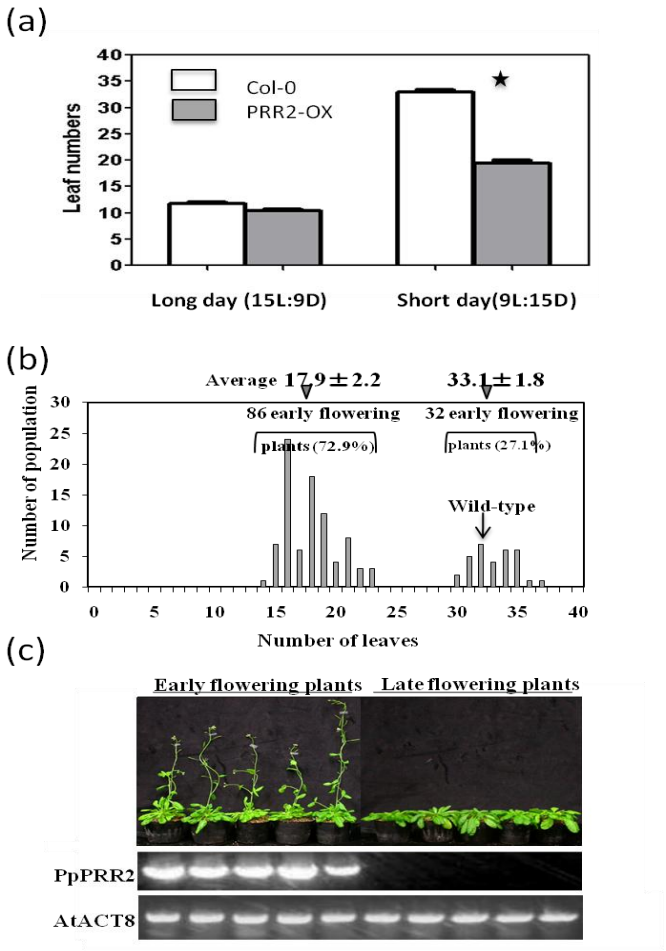

Figure 19. Disturbed regulatory pathway of the circadian clock-mediated photoperiodic control of flowering time caused by the heterologous expression of *PpPRR2* in *A. thaliana*. (a) Flowering time of four independent transgenic lines (L3, L5, L7 and L9) in long day and short day conditions. (b) A large number of T2 transgenic plants of a *PpPRR2* misexpression line (L5) (n=114) were grown under 9:15LD , and flowering time of each plant was evaluated

quantitatively by counting the number of leaves when the primary inflorescence was detected. The distribution of the populations with various leaf numbers was shown in the graph. 72.9% of them analyzed belonged to the population of early flowering plants (the mean leaf number: 17.9±2.2), and 27.1% of them belonged to the population of late flowering plants (the mean leaf number: 33.1±1.8). The result statistically indicates that the segregation ratio is 3:1 ($\chi^2 = 0.09$, $p<0.05$). The mean leaf number of wild type examined concomitantly is shown by the arrow for reference. (c) Representatives of early and late flowering plants (five each) were photographed. Transcripts from the 35S::*PpPRR2* fusion gene were examined with RT-PCR analyses. Primers used are described in Table 2D.

3.4.3 Hypocotyl elongation during early photomorphogenesis

In the above section, an early flowering phenotype was observed in *PpPRR2* misexpressing plants. Next, I compared lengths of hypocotyls in transgenic and wild type plants grown under long day (15:9LD) and short day (9:15LD) conditions. Very little or no effect was observed under long day condition on hyopcotyl lengths of both plants, however, short hypocotyls were observed under short day condition in *PpPRR2* misexpressing plants than wild type plants (Figs. 20a and 20b).

Then, the same T2 transgenic line (L5) which was studied in the above section was further subjected to the analysis of hypocotyl elongation during early photomorphogenesis. T2 seedlings were germinated and incubated on SM gellan gum plates for 7 days in short day conditions. The distribution of hypocotyl lengths was examined for a large number of T2 seedlings (Fig. 20c). The result indicates that both the homozygous and heterozygous *PpPRR2* misexpressing lines exhibit the phenotype of short hypocotyls in short day conditions, because 75% of seedlings showed the phenomenon, and remains showed the wild type length of hypocotyls on average. This statistical assumption was independently supported by Fig. 20b, in which four independent transgenic lines including L3, L5, L7, and L9 were subjected to essentially the same analyses of hypocotyl elongation. However, 10 day old seedlings which were resistant to bialaphos sodium salt (20 μM) were examined in this experiment. The results confirmed that *PpPRR2* misexpression seedlings exhibit the phenotype of short hypocotyls (Fig.

20b). It was also confirmed that every line of the drug-resistant plants with short hypocotyls expressed a large amount of *PpPRR2* transcripts (Fig. 20b). These results supported the idea that when the *PpPRR2* gene was introduced into *A. thaliana* plants, the moss gene exhibited an ability to disturb the intrinsic regulatory pathway of the short day-specific elongation of hypocotyls during photomorphogenesis of the host.

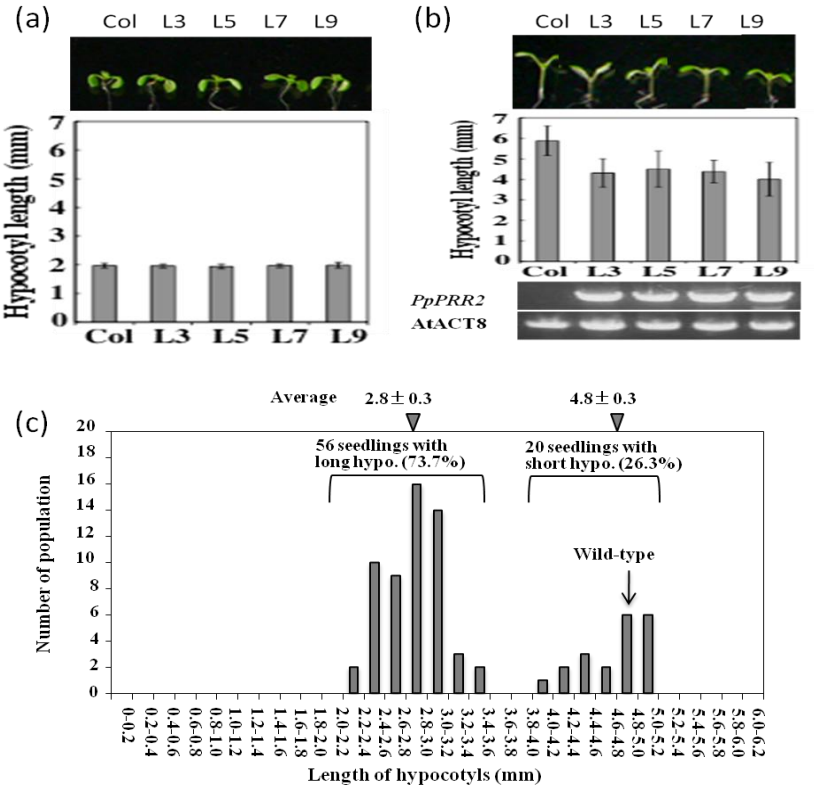

Figure 20. Disturbed intrinsic regulatory pathway of the circadian clock-controlled elongation of hypocotyls during photomorphogenesis caused by the heterologouse expression of *PpPRR2* in *A. thaliana*. (a) Four independent transgenic plants were germinated and incubated on MS gellan gum plates for 7 days under long day (15:9LD) condition and then hypocotyl lengths were measured. (b) Four independent monogenic *PpPRR2* misexpressing T2 transgenic lines (L3, L5, L7, and L9) were subjected to analysis of hypocotyl elongation under short day (9:15LD) condition. 10 day old seedlings which were resistant to bialaphos sodium salt (20 μM) were examined in this experiment. The picture of representative seedlings was shown at the top. Hypocotyl lengths of etiolated seedlings of the transgenic lines in the darkness were almost same as that of Col (data not shown). For each line, the plants which were resistant to

bialaphos sodium salt (20 μM) were grown to prepare RNA samples. They were subjected to RT-PCR analysis to detect *PpPRR2* transcripts. The results are indicated at the bottom. (c) A large number of T2 transgenic seeds of a *PpPRR2* misexpression line (L5) (n=76) were germinated and incubated on MS gellan gum plates for 7 days under 9:15LD, and then hypocotyl lengths were measured. The distribution of populations with various hypocotyl lengths was shown in the graph. 73.7% of the seedlings analyzed had shorter hypocotyls (the mean value: 2.8±0.3), and 26.3% of them had longer hypocotyls (the mean value: 4.8±0.3). The result statistically indicates that the segregation ratio is 3:1 (χ^2 = 0.09, $p<0.05$). The mean hypocotyl length of wild type examined concomitantly is shown by the arrow for reference.

3.4.4 Red light sensitivity during early photomorphonegesis

AtPRR-OX seedlings were highly sensitive to red light during early photomorphogenesis (Sato *et al*., 2002; Matsushika *et al*., 2002; Matsushika *et al*., 2007). To further compare the functions of *AtPRR*s and *PpPRR2*, I examined the effect of red light during early photomorphogenesis on *PpPRR2* misexpressing seedlings. *PpPRR2* misexpressing seedlings showed hypersensitivity towards red light resulting in shorter hypocotyls than those of wild type Col (Fig 21). However, their hypersensitivity was not observed as high as observed in *AtPRR* seedlings; however the effect on hypocotyl length was found similar (leading to shorter hypocotyls).

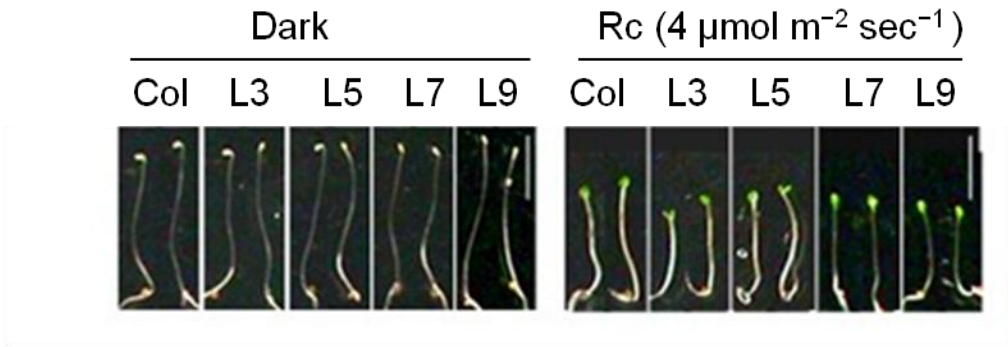

Figure 21. Effect of *PpPRR2*-misexpression on red light response during early photomorphogenesis. Four independent transgenic plants seeds were sown on four layers of

filter paper (Fankhauser and Casal, 2004) and allowed to imbibe in sterile water in the dark for 48 hours at 4°C. Then, seeds were exposed to white light for 6 hours in order to enhance germination, followed by incubation at 22°C for 18 hours again in the dark. Plants were grown for 72 hours under LL with a fluence rate of 4 µmol m^{-2} sec^{-1} or in the dark (control).

Above results clearly showed functional conservation of the clock-associated gene (*PpPRR2*) in the early land plant *P. patens* and the higher plant *A. thaliana*. Phenotypes of *A. thaliana* plants misexpressing *AtPRR5/7/9* and *PpPRR2* are summarized in Table 3.

Table 3. Summarized view of the phenotypes of transgenic plants misexpressing or overexpressing *PRR*s.

Transgenic plants	Period of free running rhythms	Flowering time (Short day conditions)	Red light sensitivity (Elongation of hypocotyls)	References
AtPRR5-OX	Damp (low amplitude)	Early	Hyper	Sato *et al*., 2002
AtPRR7-OX	Long	Early	Hyper	Matsushika *et al* Farre *et al*., 2007
AtPRR9-OX	Short	Early	Hyper	Matsusika *et al*., 2002
***PpPRR2*-OX**	**Short**	**Early**	**Hyper**	**This study**

4. DISCUSSION

4.1 Evolution and divergence of *PRR* genes in green plants

PRR genes have been found in all green plants so far examined, but not in animals and prokaryotes. I have isolated four *PRR* homologs from the moss *P. patens*: *PpPRR1, PpPRR2, PpPRR3* and *PpPRR4*. No more genes as closely related to *A. thaliana PRR*s as these four genes were detected in *P. patens* by extensive genome sequence analysis. Based on protein sequence homology it was discovered that *PRR* genes from green algae *O. tauri* to *A. thaliana* shared significant homology on two highly conserved motifs RLD and CCT domain. Interestingly, all *PpPRR*s found to be unique to retain phsphoacceptor aspartic acid (D) residue on the RLD domain, in contrast to all flowering plant counterparts studied so far, which has glutamic acid (E) residue at that position. In *in-vitro* assay, the PpPRR2 RLD peptide underwent phosphotransfer (Fig. 12), consistent with its complete DDK motif (Figs. 8a, 8c), strongly suggesting that PpPRR2 functions as an RR. Besides, according to phylogenetic analysis (Fig. 9), PpPRRs are phylogenetically closely related to angiosperm PRRs. Therefore, it is presumed that the similarity of RLDs of PRRs to the authentic receiver domain is not only superficial but that PRRs were certainly derived from an authentic RR. Most probably, higher plant PRRs have lost their phosphorelay function through the course of evolution, largely due to the substitution of the phosphoacceptor aspartic acid to a glutamic acid in their RLDs, and other critical residues such as the first aspartic acid of the DDK motif should have concomitantly diverged. Importantly, the *O. tauri* OtTOC1 and the *C. reinhardtii* CrPRR2 also share not only the potential phosphoacceptor aspartic acid but also the entire DDK motif (Fig. 8a; see Corellou *et al*., 2009, Satbhai *et al*., 2010). Although there has so far been no report about whether or not these algal proteins undergo phosphotransfer, they are also assumed to function as RRs, representing prototypic proteins of the land plant PRRs.

In this study, I have presented evolutionary explanations not only for the origin but also for the diversity of *PRRs* in land plants (Fig. 22). The pattern of phylogenetic tree indicates that

the TOC1/PRR1 group first diverged, and then split the PRR9/5 group and the other branch, the latter containing the PRR7/3 group. Since PpPRRs are positioned inside the branch containing the PRR7/3 group, the origins of the TOC1 and PRR9/5 groups date back before the divergence of moss from higher plant lineages. The ancient origin of the TOC1 group is supported by the observation that *C. reinhardtii* and *C. variabilis* seem to have a TOC1 ortholog (Fig. 9). Furthermore, since the cluster of PpPRRs and lycophyte SmPRR7a/7b is sister to all the angiosperm PRR7/3 sequences (Fig. 9), the divergence between the PRR7/3 group and the ancestor of PpPRRs and SmPRR7a/7b also predates the divergence of moss from higher plants. Therefore, the common ancestor of moss and higher plants possessed *TOC1*, *PRR7/3* and *PRR9/5* orthologs in its genome, but these genes appear to have been lost later within the moss lineage (Fig. 22). In the lycophyte lineage, *PRR7/3* and *PRR9/5* orthologs have been lost and the unique combination of the *TOC1* (*SmTOC1*) and *PpPRR* (*SmPRR7a/7b*) orthologs still now remain (Fig. 22). In the angiosperm lineage, only *PpPRR* ortholog(s) has been lost, resulting in the current three *PRR* groups (Fig. 22). Concerning the timings of substitution of the phosphoacceptor residue, there are two alternative explanations. In one scenario (Fig. 22a), the phosphoacceptor aspartic acid residue of the PpPRRs and SmPRR7a/7b can be traced back to that found in the algal sequences; the phosphoacceptor residue in these sequences has never been substituted. This explanation might seem simple and more likely; however, if this were the case, the aspartic acid residue must have been substituted, according to the branching patterns of our tree, independently within each lineage of the *TOC1*, *PRR7/3* and *PRR9/5* groups (Fig. 9 and 22a). In another scenario (Fig. 8b), simpler at least in terms of the frequency of substitutions, the aspartic acid was substituted only once to a glutamic acid before the divergence of all the PRR subfamilies. In this case, an aspartic acid was regained by a second substitution in the ancestral lineage of *PpPRRs* and two lycophyte genes (Fig. 22b). If this were the case, *PpPRR1* might be, again, in the process of divergence from authentic RR-type sequences. In order to know which hypothesis, or yet another scenario, is more plausible, more sequence data is needed; in particular, *PRR* sequences should be characterized from other primitive plants, *i.e.*, liverworts, hornworts, ferns and gymnosperms.

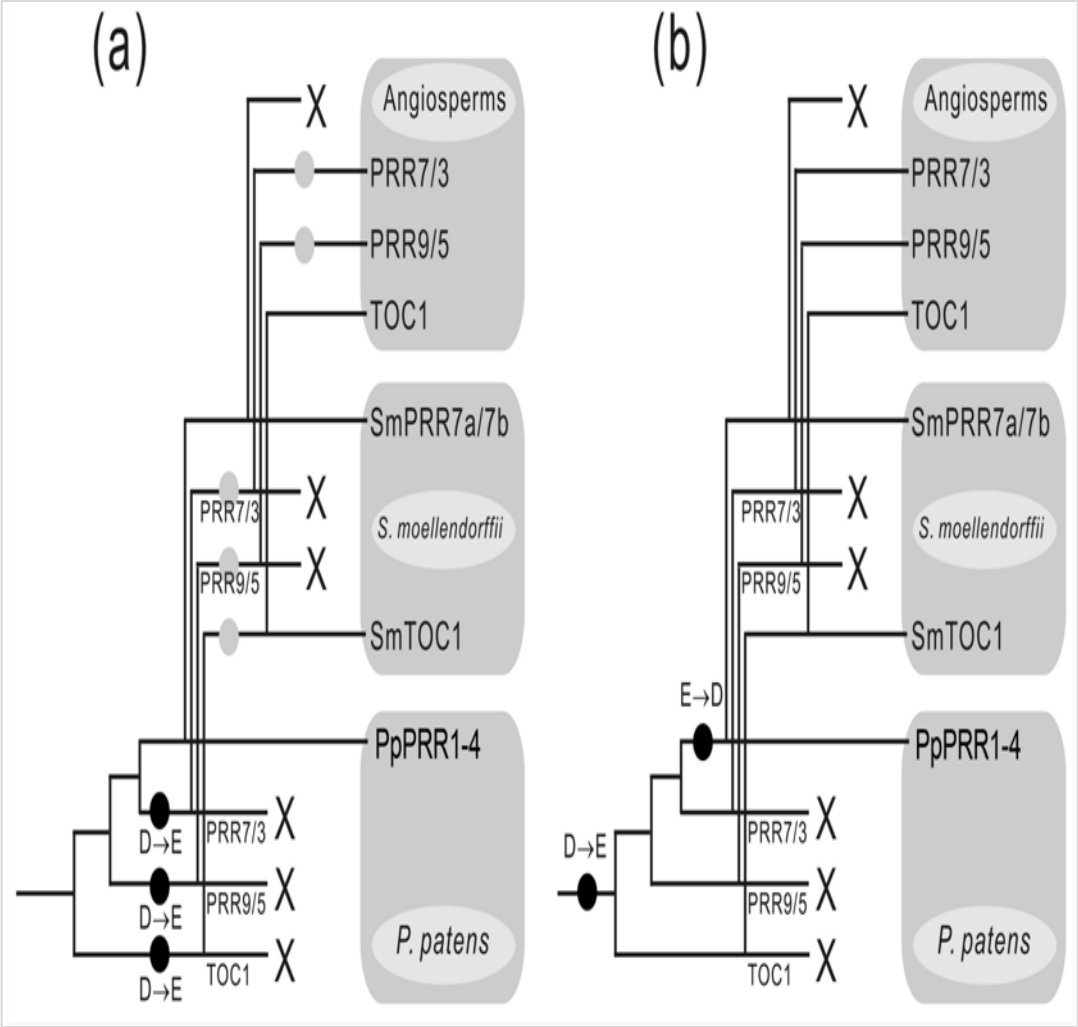

Figure 22. Evolutionary scenarios for divergence of *PRR* genes in land plants. Two alternative explanations are presented: (a) scenario in which the phosphoacceptor aspartic acid residue in PpPRR and SmPRR7a/7b sequences has never been substituted, and (b) scenario in which the aspartic acid was substituted to glutamic acid only once and it was regained by a second substitution in the ancestral lineage of *PpPRRs* and two lycophyte genes. Closed circles represent amino acid substitution events at the potential phosphoacceptor residue. Grey circles represent alternative timings of amino acid substitutions indicated by the closed circles. Crosses represent gene loss events.

4.2 Transcriptional regulation of *PpPRR* genes

In this study, I demonstrated diurnal regulation of *PpPRR1, PpPRR2, PpPRR3*, and *PpPRR4* expression, with a broad peak in expression during the day and a trough during the night. The increase in transcript abundance was observed soon after dawn, and maximum levels were reached within 8-12 hours, for all *PpPRR* genes (Fig. 13a). The strong increase in *PpPRR*s transcript abundance at dawn, together with the increase shortly before dawn in case of *PpPRR1* and *PpPRR3*, suggests *PpPRR*s expression is regulated by light as well as circadian clock. The most reliable diagnostic feature of circadian rhythms is that they persist under continuous conditions (Johnson, 2001). In continuous light conditions, expression levels of all *PpPRR*s remained high and became arrhythmic, consistent with a direct and positive responsiveness to light (Fig 13c). However, in extended darkness, expression levels increased after initial decreases and clearly showed circadian rhythms. Taken together, the data indicate that the diurnal expression pattern of *PpPRR*s is achieved by a direct response to light signaling, and response to an endogenous timekeeper becomes clear only in the absence of light.

Although the molecular identity of a putative *P. patens* circadian clock is still unclear, several clock-associated genes have been analyzed to date. Interestingly, the expression of each clock-associated gene, *PpLhcb2, PpCOL1, PpSig5, psbD, PpCCA1a* and *PpCCA1b* only showed significant rhythmicity in continuous darkness, not in continuous light (Aoki *et al*., 2004; Ichikawa *et al*., 2004; Shimizu *et al*., 2004; Okada *et al*., 2009). This is in contrast with their respective *A. thaliana* homologs, the transcript levels of which continue oscillating in continuous light for several cycles (Hicks *et al*., 1996; Schaffer *et al*., 1998; Wang and Tobin *et al*., 1998). Now, my analysis offers four additional examples of *P. patens* clock-associated genes whose expression reveals circadian control only in conditions of continuous darkness. This is again in contrast with related genes in *A. thaliana*; *TOC1/PRR1, PRR3, PRR5, PRR7* and *PRR9*, which all continue cycling in continuous light conditions (Makino *et al*., 2002; Sato *et al*., 2002; Murakami *et al*., 2004; Matsushika *et al*., 2005; Mizuno 2005; Farre *et al*., 2007). Taken together, these observations possibly reflect fundamental differences in the responses of the *P. patens* and *A. thaliana* clocks to light.

Interestingly, all the above mentioned *P. patens* clock-associated genes, including *PpPRR1, PpPRR2, PpPRR3* and *PpPRR4*, respond to continuous light and dark conditions in a similar way as *Light-Harvesting Complex-b* (*Lhcb1.1*) and another circadian marker gene, *Cold-Circadian Rhythm-RNA Binding2* (*CCR2*), and *Chlorophyll A/B-Binding1* (*CAB1*) in the *A. thaliana* photoperiod insensitive *early-flowering 3* (*elf3*) mutant (Covington *et al*., 2001, Hicks *et al*., 1996; McWatters *et al*., 2000). Normally, *Lhcb1.1* expression levels oscillate in continuous light and in continuous darkness (Millar and Kay, 1996), as mentioned above, whereas in the *elf3* mutant, rhythmicity is maintained in continuous darkness (Covington *et al*., 2001), but lost in continuous light (Hicks *et al*., 1996). The conditional arrhythmic phenotype suggests that the circadian pacemaker is intact in darkness in *elf3* mutant plants, but the transduction of light signals to the circadian clock is impaired (Hicks *et al*., 1996). Possibly, the *P. patens* clock resembles the clock of the *A. thaliana elf3* mutant in its inability to modulate light signaling in continuous light conditions. In *P. patens,* other clock-controlled genes will have to be investigated to confirm this. Homologs of the *A. thaliana CCR2* gene would be good candidates, because in *A. thaliana* expression of the *CCR2* gene shows a robust circadian rhythm in both continuous light and continuous darkness (Kreps and Simon, 1997; Strayer *et al*., 2000). Interestingly, presence of an *ELF3* homolog (*PpELF3*) in *P. patens* further increases complexity about *ELF3* function (Table 1). Possibly, *PpELF3* functions are more diverged than flowering plant counterparts (Table1, Holm *et al*., 2010). In future, the *PpELF3* gene should be characterized in order to address this issue.

To further study *PpPRR*s regulation by light, experiments were designed to analyze the induction of *PpPRR* genes by different types of light (Fig.16). The expression of each gene responded to white light, blue light, and red light, suggesting responsiveness to integrated light signaling, rather than light signaling through a particular photoreceptor. The light perceiving photoreceptors of *P. patens* have been characterized and were shown to belong to the same three major classes of photoreceptors that are found in *A. thaliana*: the red/far-red light perceiving phytochromes, the blue/UV-A light perceiving cryptochromes and phototropins. Each of the *P. patens* photoreceptors has been functionally studied by gene targeting strategy. Phytochromes were implicated in mediating phototropism, polarotropism and chloroplast movement (Mittmann *et al*., 2004). Phototropins were shown to be involved in chloroplast movement (Kasahara *et al*., 2004). Cryptochromes were found to regulate many steps in moss development, *e.g.,* branching

of protonema filaments and gametophore development, partly by controlling auxin signal transduction (Imaizumi *et al*., 2002). Taken together, the same classes of photoreceptors that regulate light-dependent processes in *A. thaliana* are also key regulators of light-dependent developmental and physiological processes in *P. patens*. Further investigation of this issue may include analyzing the expression of *PpPRR* genes in the different *P. patens* photoreceptor mutants.

Among the *A. thaliana PRR* family members, *AtPRR9* gene is unique in that its expression is rapidly induced by light at the level of transcription (Ito *et al*., 2003). *AtPRR9* gene appears to play a crucial role in or close to the circadian clock and light-signal transduction pathways (Matsushika *et al*., 2002; Sato *et al*., 2002; Ito *et al*., 2003). My analyses on *PpPRR* expression clearly showed similar light responses as *AtPRR9*, which further strengthen the similarities among *PRR*s from two distantly related species. Every *PRR* gene from a flowering plant that has been analyzed to date displayed diurnal or circadian rhythms in transcript abundance (Makino *et al*., 2002; Sato *et al*., 2002; Murakami *et al*., 2004; Matsushika *et al*., 2005; Mizuno 2005; Farre *et al*., 2007). Together with the findings for *PpPRR1, PpPRR2, PRR3,* and *PpPRR4,* it is suggested that circadian/diurnal regulation of transcription is a generally conserved feature of *PRR* genes. These observations are consistent with the notion that *PRR* genes may have widely conserved roles in light signal transduction, and circadian rhythms (Matsushika *et al*., 2002a; Sato *et al*., 2002; Makino *et al*., 2002; Kaczorowski and Quail, 2003).

4.3 Intraspecific divergences among the *PpPRR* genes

Results obtained in this study consistently demonstrate intraspecific divergences among the *PpPRR* genes. The phylogenetic tree (Fig. 9), intron insertion sites (Fig. 11) and expression profiles (Figs. 13, 14, and 15) and differential expression by light (Fig. 16) suggests the divergence between *PpPRR1/PpPRR3* and *PpPRR2/PpPRR4*. The *A. thaliana PRR* family members show differentially regulated expression profiles, reflecting the fact that they act at different nodes in the circadian network and are functionally diverged from one another (Fig. 2,

Mizuno and Nakamichi 2005; Mizuno, 2005). Therefore, *PpPRR1/PpPRR3* and *PpPRR2/PpPRR4* are also predicted to be functionally diverged. In a previous study, Holm *et al*. did not detect any differential expression among the four *PpPRR* genes in a light-dark cycle followed by DD (Holm *et al*., 2010). This may be because their light-dark regime is different from mine: they used a long day regime, a 16-hour light 8-hour dark cycle, whereas mine is a 12-hour light 12-hour dark cycle(s) (12:12LD; Figs 13 and 14). All *PpPRRs* are induced by light (Fig. 16), and this light responsiveness may have apparently synchronized the trough phases of *PpPRRs* with the earlier dawn in the short night of their long day regime, whereas difference in trough phases between *PpPRR1/PpPRR3* and *PpPRR2/PpPRR4* are obvious in our longer nights (Fig. 13a).

On the other hand, the results of the *in-vitro* assay (Fig. 12) and detailed sequence comparison (Fig. 8a) suggests that PpPRR2/PpPRR3/PpPRR4 function as RRs, whereas PpPRR1 does not or its phosphotransfer ability is very weak. The moss *PpPRR*s, if not all of them, are anticipated to have some clock-associated functions as do *A. thaliana* PRRs, from the following facts: 1) the circadian networks of *A. thaliana* and *P. patens* are predicted to be at least partially conserved (Okada *et al*., 2009) and 2) *O. tauri*, which belongs to green algae, the closest relative of land plants, has a *PRR* homolog that functions as a clock gene (Corellou *et al*., 2009). Since RRs are generally involved in signaling cascades responsive to environmental/endogenous signals, *PpPRR2/PpPRR4* might function, rather than in the core clock circuitry, in an input pathway(s) that must be responsive to environmental cues such as light and temperature.

4.4 Functional conservation of *PRR*s

Recently, clock-related homologs with essentially conserved expression profiles have been isolated from several plant species (Boxall *et al*., 2005; Ramos *et al*., 2005; Murakami *et al*., 2007; Serikawa *et al*., 2008). These studies suggest that, the basic clock components of circadian systems are likely conserved among flowering plants. Very recently, Corellou *et al*. (2009) identified two functional homologs of higher plant core clock genes, namely *PRR-like* and

CCA1-like, in green algae *O. tauri*. However, very little is known about functional conservation of clock-associated genes in lower land plants.

As reported before several clock-associated components in *P. patens* (*PpCCA1a*, *PpCCA1b*, *PpPRRs*, *PpLUX*, *PpELF3*, and *PpELF4*) were investigated, which would be orthologs of the circadian clock components in *A. thaliana* (Table 2, Holm *et al*., 2010). It was also found that the putative clock-associated genes of *P. patens* displayed rhythmic expression profiles at the level of transcription in continuous dark (Okada *et al*., 2009a). These results suggested that circadian clock system of bryophyte is similar to that of flowering plants (Okada *et al*., 2009; Prigge *et al*., 2010). Recently, Okada *et al*. reported that *PpCCA1a* and *PpCCA1b* are functional counterparts of *AtCCA1/LHY*.

In this study, it was demonstrated that the putative clock gene *PpPRR2* of *P. patens* exhibited an ability to modify the intrinsic mechanisms underlying the circadian clock and its output pathways in *A. thaliana*, provided that the *PpPPR2* gene was misexpressed even in the evolutionarily divergent host. Transgenic plants thereby exhibited the phenotypes of short period rhythm in continuous dark, early flowering in short day, short hypocotyls in short day and hypersensitivity to red light during early photomorphogenesis, compared with the host plants. Considering the fact that the similar events were previously observed when the *A. thaliana* clock-associated *PRR* genes (*e.g*., *PRR9*) were misexpressed (Table 3, Matsushika *et al*., 2007), it is speculated that the *PpPRR2* gene plays a clock-associated role in the *P. patens*. The results of this study also support the view that plant *PRR*s are indeed the evolutionarily conserved crucial clock components. To further confirm this idea; more direct experiments are prerequisite, including characterization of multiple loss-of-function mutants of *PpPRRs* in the *P. patens*.

4.5 Simplified circadian clock network model of *P. patens*

As mentioned in Introduction section, the current *A. thaliana* clock models hypothesize several interlocked loops that contain both negative and positive regulatory elements that control gene transcription (Fig. 2, Locke *et al*., 2006; McClung, 2006; Harmer, 2009). As compare to the

A. thaliana clock models, a *P. patens* model is thought to be less complex as several homolog of *A. thaliana* clock component are absent in *P. patens* (*TOC1*, *GI*, and *ZTL*). TOC1 and GI comprise a feed-back loop, also referred to as the evening-phased loop. Moreover, *ZTL* also plays roles in *A. thaliana* clock with close relationship to *TOC1* and *GI* (Kim *et al*., 2009).

By summarizing results obtained in this study and our group's previous reports, I would like to propose the simplified clock model of *P. patens* (Fig. 23).

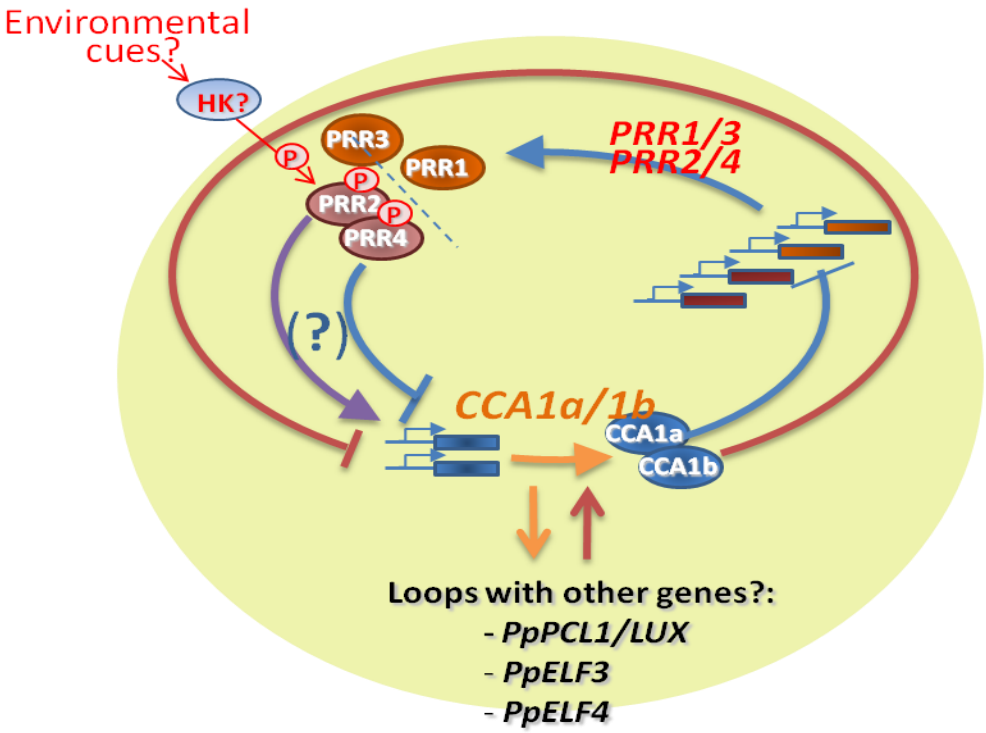

Figure 23. A simplified version of the *P. patens* circadian clock network. Proposed single loop model comprising homologs of two core clock components *PpCCA1a/1b* and *PpPRR*s based on this study (Satbhai *et al*., in press) and recent analyses (Okada *et al*., 2009a). See the main text for details.

As reported previously *PpCCA1a/1b* repress their own expression by forming negative feedback loop (Okada *et al*., 2009). This study further revealed that *PpCCA1a/1b* control the expression of *PpPRR*s (Fig. 17). Positive or possibly negative regulation of *PpCCA1a/1b* by *PpPRRs* is still unclear. Moreover, a His-Asp phosphorelay system might have a key role(s) in *P. patens* circadian clock as RR features and phosphotransfer ability of *PpPRR*s were shown in this study. However, it was shown that double disruptants of *PpCCA1a* and *PpCCA1b* in the moss still display rhythmic output of the *PpPRR1* (Okada *et al*., 2009). This suggests the presence of further components, and/or possibly additional unknown loops, other than a proposed single loop, that contribute to the maintenance of endogenous circadian rhythms in *P. patens*. Therefore, additional clock associated components found in *P. patens* (*PpPCL1/PpELF3/PpELF4*) might have key roles in the *P. patens* clock. In conclusion, two highly diverged species *P. patens* and *A. thaliana* clock model comprised similar clock associated components which suggests that conservation of core clock machineries. Nevertheless, several key differences are also observed which are due to long evolutionary history between *P. patens* and *A. thaliana*. Results obtained in this study may indicate that the *P. patens* clock system represents ancestral properties in contrast to the more complex nature of higher plant *A. thaliana* clock system. These findings lay the foundation to understand the evolution of plant circadian systems.

5. SUMMARY

The *PRR* genes play a central role in the flowering plant *A. thaliana* circadian clock. To address the question of the origin of *PRRs*, this gene family was analyzed in the moss *P. patens,* a phylogenetically distant plant.

In *A. thaliana*, five *PRR* homologs exist (*TOC1/PRR1, PRR3, PRR5, PRR7, and PRR9*). Four PRR homologs were found in *P. patens*, suggesting that this gene family has ancient origins in the plant kingdom. Phylogenetic analyses demonstrated that all PpPRRs form a separate cluster in phylogenetic trees and they showed a close relationship with the higher plant PRR7/3 group. A striking finding is that *P. patens* is unique in that *TOC1* ortholog is absent. Another striking difference found in PpPRRs is that they all retained the potential phosphoacceptor residue similarly as RRs. Consistent with this, the PpPRR2 protein underwent phosphotransfer in an *in-vitro* assay.

An essential feature of *PRR*s functioning in *A. thalaina* is circadian rhythms of transcript abundances. *PpPRR*s are also found to be under the control of circadian clock, and they all showed robust diurnal rhythms in 12:12LD and endogenous circadian rhythms in DD conditions. Interestingly, the expression of each *PpPRR* gene only showed significant rhythmicity in DD, but not in LL. This is in contrast with their respective *A. thaliana* homologs, the transcript levels of which showed robust circadian rhythms in LL. Moreover, all *PpPRR*s showed acute light responses to three different types of light, suggesting their role in light signaling.

In the *PpCCA1a/ PpCCA1b* double disruptant, all *PpPRR*s showed higher expression in light than in WT, suggesting their expression was suppressed by *PpCCA1a/PpCCA1b* in the presence of light. Similar negative regulation of *PpPRR*s by *PpCCA1a/PpCCA1b* was already found in their *A. thaliana* counterparts, suggesting the conservation of clock systems in two distantly related species.

The functional similarities of *PpPRR*s and *AtPRR*s were assessed by misexpressing *PpPRR2* gene in *A. thaliana. PpPRR2* misexpressing *A. thaliana* plants exhibited the phenotypes of a short period rhythm in DD, early flowering in short day, short hypocotyls in short day and

hypersensitivity to red light during early photomorphogenesis, compared with WTs. Similar events were previously demonstrated when the *A. thaliana PRRs* were misexpressed. These similarities provide supportive evidence that these genes in the two species have similar functions as clock components. Therefore, the genetic structures of the circadian oscillators are likely conserved between early land plant and flowering plants; in short the core clock components of circadian systems are, at least in part, likely conserved among land plants.

The results of this study clearly supported the view that plant *PRR*s are indeed the evolutionarily conserved crucial clock components. In parallel, however, there appears to be critical functional divergences in plant *PRRs*. To further confirm this idea; more direct experiments are required, including characterization of multiple loss-of-function mutants of *PpPRRs* in the moss. In a future study, in parallel with gene knock out experiments, it should also be addressed whether PpPRRs are involved in phosphotransfer functions *in planta*. Moreover, a HK(s) and a HPt(s) that are partners to (at least some of) PpPRR proteins should be characterized. It might not be easy to identify a partner HK(s) because the *P. patens* genome contains as many as ~31 HK sequences (Ishida *et al*., 2010), unlike *A. thaliana*, which contains only 8 HK genes (Hwang *et al*., 2002). However, the availability of the entire genome sequence, many full-length cDNA clones and the feasibility of gene functional analysis based on gene targeting techniques will support the identification of such HK and HPt genes in *P. patens*, possibly as novel clock genes.

6. REFERENCES

Alabadí D, Oyama T, Yanovsky MJ, Harmon FG, Más P, Kay SA. 2001. Reciprocal regulation between TOC1 and LHY/CCA1 within the *Arabidopsis* circadian clock. *Science* 293:880-883.

Altschul, S.F., Madden, T.L., Schaffer, A.A., Zhang, J., Zhang, Z., Miller, W.,and Lipman, D.J. 1997. Gapped BLAST and PSI-BLAST: a new generation of protein database search programs. *Nucleic Acids Res*. 25: 3389-3402.

Anderson SL, Somers DE, MillarAJ, Hanson K, Chory J, and Kay SA. 1997. Attenuation of phytochrome A and B signaling pathways by the Arabidopsis circadian clock. *Plant Cell*. 9: 1727-1743.

Ashton NW, Cove DJ. 1977. The isolation and preliminary characterization of auxotrophic and analogue resistant mutants in the moss *Physcomitrella patens*. *Mol. Gen. Genet.* 154: 87–95.

Azuma N, Kanamaru K, Matsushika A , Yamashino T, Mizuno T, Kato M, Kobayashi T. 2007. *In vitro* analysis of His-Asp phosphorelays in *Aspergillus nidulans*: the first direct biochemical evidence for the existence of His-Asp phosphotransfer systems in filamentous fungi. *Biosci. Biotechnol. Biochem.* 71: 2493-2502.

Bowman JL, Floyd SK, Sakakibara K. 2007. Green genes-comparative genomics of the green branch of life. *Cell* 129: 229-234.

Boxall SF, Foster JM, Bohnert HJ, Cushman JC, Nimmo HG, Hartwell J. 2005.Conservation and divergence of circadian clock operation in a stress-inducible Crassulacean acid metabolism species reveals clock compensation against stress. *Plant Physiol*.137: 969-82.

Clough, S.J., and Bent, A.F. 1998. Floral dip: a simplified method for Agrobacterium-mediated transformation of Arabidopsis thaliana. *Plant J*.16: 735-743.

Corellou F, Schwartz C, Motta JP, Djouani-Tahri el B, Sanchez F, Bouget FY. 2009. Clocks in the green lineage: comparative functional analysis of the circadian architecture of the picoeukaryote ostreococcus. *Plant Cell* 21: 3436-3449.

Covington, M.F., Panda, S., Liu, X.L., Strayer, C.A., Wagner, D.R., and Kay,S.A. 2001. ELF3 modulates resetting of the circadian clock in Arabidopsis. *Plant Cell* 13: 1305-1315.

Devlin, P.F. 2002. Signs of the time: environmental input to the circadian clock. *J Exp Bot*. 53: 1535-1550.

DOE Joint Genome Institute. 2007. *P. patens* subsp *patens* V1.1, http://genome.jgi-psf.org//Phypa1_1/Phypa1_1.home.html.

Edmunds LN. 1988. Cellular and molecular bases of biological clocks. New York: Springer

Fankhauser C and Casal J. 2004. Phenotypic characterization of a photomorphogenic mutant. *Plant J*. 39:747-60.

Farre EM, Harmer SL, Harmon FG, Yanovsky MJ, Kay SA. 2005. Overlapping and distinct roles of PRR7 and PRR9 in the *Arabidopsis* circadian clock. *Curr. Biol.* 15: 47–54.

Farré EM, Kay SA. 2007. PRR7 protein levels are regulated by light and the circadian clock in Arabidopsis. *Plant J*. 52: 548-60.

Felsenstein J. 1985. Confidence limits on phylogenies: An approach using the bootstrap. *Evolution* 39: 783-791.

Fujiwara S, Wang L, Han L, Suh SS, Salome PA, McClung CR, Somers DE. 2008. Post-translational regulation of the *Arabidopsis* circadian clock through selective proteolysis and phosphorylationof pseudo-response regulator proteins. *J. Biol. Chem.* 283: 23073–23083.

Hamilton EE, Kay SA. 2008. SnapShot: circadian clock proteins. *Cell*, 135: 368-368.

Harmer SL. 2009. The circadian system in higher plants. *Annu. Rev. Plant. Biol*. 60: 357-377.

Hazen SP, Schultz TF, Pruneda-Paz JL, Borevitz JO, Ecker JR, Kay SA. 2005. LUX ARRHYTHMO encodes a Myb domain protein essential for circadian rhythms. *Proc Natl Acad Sci U S A*. 102: 10387-92.

Hecht V, Foucher F, Ferrándiz C, Macknight R, Navarro C, Morin J, Vardy ME, Ellis N, Beltrán JP, Rameau C, Weller JL. Conservation of *Arabidopsis* flowering genes in model legumes. *Plant Physiol.* 137: 1420-1434.

Hecht V, Knowles CL, Vander Schoor JK, Liew LC, Jones SE, Lambert MJ, Weller JL. 2007. Pea *LATE BLOOMER1* is a *GIGANTEA* ortholog with roles in photoperiodic flowering, deetiolation, and transcriptional regulation of circadian clock gene homologs. *Plant Physiol.* 144: 648-661.

Hicks KA, Millar AJ, Carre IA, Somers DE, Straume M, Meeks-Wagner DR, and Kay SA. 1996. Conditional circadian dysfunction of the Arabidopsis early-flowering 3 mutant. *Science*. 274: 790-792.

Higgins DG, Sharp PM. 1988. CLUSTAL: a package for performing multiple sequence alignment on a microcomputer. *Gene* 73: 237-244.

Holm K, Källman T, Gyllenstrand N, Hedman H, Lagercrantz U. 2010. Does the core circadian clock in the moss *Physcomitrella patens* (Bryophyta) comprise a single loop? *BMC Plant Biol.* 10: 109.

Ichikawa K, Sugita M, Imaizumi T, Wada M, Aoki S. 2004. Differential expression on a daily basis of plastid sigma factor *PpSig* genes from the moss *Physcomitrella patens*: Regulatory interactions among *PpSig5*, the circadian clock and blue light signaling mediated by cryptochromes. *Plant Physiol.* 136: 4285-4298.

Imaizumi, T, Kadota, A, Hasebe, M, and Wada, M. 2002. Cryptochrome light signals control development to suppress auxin sensitivity in the moss Physcomitrella patens. *The Plant Cel.l* 14: 373-386.

Ishida K, Yamashino T, Yokoyama A, Mizuno T. 2008. Three type-B response regulators, ARR1, ARR10 and ARR12, play essential but redundant roles in cytokinin signal transduction throughout the life cycle of *Arabidopsis thaliana*. *Plant Cell Physiol.* 49: 47-57.

Ishida K, Niwa Y, Yamashino T, Mizuno T. 2009. A Genome-Wide Compilation of the Two-Component Systems in *Lotus japonicas*. *DNA Res*. 16: 237–247.

Ito S, Matsushika A, Yamada H, Sato S, Kato T, Tabata S, Yamashino T, Mizuno T. 2003. Characterization of the APRR9 pseudo-response regulator belonging to the APRR1/TOC1 quintet in Arabidopsis thaliana. *Plant Cell Physiol*. 44:1237-45.

Jones DT, Taylor WR, Thornton JM. (1992) The rapid generation of mutation data matrices from protein sequences. *Comput. Appl. Biosci.* 8: 275-282.

Kasahara M, Kagawa T, Sato Y, Kiyosue T, and Wada M. 2004. Phototropins mediate blue and red light-induced chloroplast movements in Physcomitrella patens. *Plant Physiol* 135: 1388-1397.

Kaczorowski KA, and Quail PH. 2003. Arabidopsis PSEUDO-RESPONSE REGULATOR7 Is a Signaling Intermediate in Phytochrome-Regulated Seedling Deetiolation and Phasing of the Circadian Clock. *Plant Cell*, 15: 2654-2665.

Kikis EA, Khanna R, Quail PH. 2005. ELF4 is a phytochrome-regulated component of a negative-feedback loop involving the central oscillator components CCA1 and LHY. *Plant J.* 44: 300-13.

Kojima S, Banno H, Yoshioka Y, Oka A, Machida C and Machida Y. 1999. A binary vector plasmid for gene expression in plant cells that is stably maintained in Agrobacterium cells. *DNA Res*. 6: 407-410.

Kreps JA and Simon AE. 1997. Environmental and genetic effects on circadian clock-regulated gene expression in Arabidopsis. *Plant Cell*. 9: 297-304.

Lang D, Zimmer AD, Rensing SA, Reski R. 2008. Exploring plant biodiversity: the *Physcomitrella* genome and beyond. *Trends Plant Sci.* 13: 542-549.

Liu H, Wang H, Gao P, Xü J, Xü T, Wang J, Wang B, Lin C, Fu YF. 2009. Analysis of clock gene homologs using unifoliolates as target organs in soybean (*Glycine max*). *J. Plant Physiol.* 166: 278-289.

Locke JC, Kozma-Bognár L, Gould PD, Fehér B, Kevei E, Nagy F, Turner MS, Hall A, Millar AJ. 2006. Experimental validation of a predicted feedback loop in the multi-oscillator clock of *Arabidopsis thaliana*. *Mol. Syst. Biol.* 2: 59.

Lowry OH, Rosebrough NJ, Farr AL, Randall RJ. 1951. Protein measurement with the Folin phenol reagent. *J. Biol. Chem.* 193: 265-275.

Makino S, Kiba T, Imamura A, Hanaki N, Nakamura A, Suzuki T, Taniguchi M, Ueguchi C, Sugiyama T, Mizuno T. 2000. Genes encoding pseudo-response regulators: insight into His-to-Asp phosphorelay and circadian rhythm in *Arabidopsis thaliana*. *Plant Cell Physiol.* 41: 791-803.

Makino S, Matsushika A, Kojima M, Yamashino T, Mizuno T. 2002. The APRR1/TOC1 quintet implicated in circadian rhythms of *Arabidopsis thaliana*: I. Characterization with APRR1-overexpressing plants. *Plant Cell Physiol.* 43: 58-69.

Más P, Kim WY, Somers DE, Kay SA. 2003. Targeted degradation of TOC1 by ZTL modulates circadian function in *Arabidopsis thaliana*. *Nature* 426: 567–570.

Matsushika A, Murakami M, Ito S, Nakamichi N, Yamashino T, and Mizuno T. 2007. Characterization of Circadian-associated pseudo-response regulators: I. Comparative studies on a series of transgenic lines misexpressing five distinctive PRR Genes in Arabidopsis thaliana. *Biosci. Biotechnol. Biochem.*, 71: 527-534.

McClung CR. 2001. Circadian rhythms in plants. *Annu. Rev. Plant Physiol. Plant Mol. Biol.* 52: 139–162.

McClung CR, Plant circadian rhythms. 2006. *The Plant Cell* 18: 792-803.

Millar AJ, Straume M, Chory J, Chua NH, Kay SA. 1995. The regulation of circadian period by phototransduction pathways in *Arabidopsis*. *Science* 267: 1163-1166.

Millar, A.J., Carre, I.A., Strayer, C.A., Chua, N.H. and Kay, S.A. 1995. Circadian clock mutants in Arabidopsis identified by luciferase imaging. *Science*, 267: 1161–1163.

Millar AJ, and Kay SA. 1996. Integration of circadian and phototransduction pathways in the network controlling CAB gene transcription in Arabidopsis. *Proc Natl Acad Sci USA*. 93: 15491-15496.

Miwa K, Serikawa M, Suzuki S, Kondo T, Oyama T. 2006. Conserved expression profiles of circadian clock-related genes in two *Lemna* species showing long-day and short-day photoperiodic flowering responses. *Plant Cell Physiol.* 47: 601-612.

Mittmann F, Brucker G, Zeidler M , Repp A , Abts T , Hartmann E , and Hughes J. 2004. Targeted knockout in Physcomitrella reveals direct actions of phytochrome in the cytoplasm. *Proc. Natl. Acad. Sci. USA*. 101: 13939-13944.

Mizuno T. 2005. Two-component phosphorelay signal transduction systems in plants: from hormone responses to circadian rhythms. *Biosci. Biotechnol. Biochem.* 69: 2263-2276.

Mizuno T, Nakamichi N. 2005. Pseudo-Response Regulators (PRRs) or True Oscillator Components (TOCs). *Plant Cell Physiol*. 46: 677-685.

Murakami M, Ashikari M, Miura K, Yamashino T, Mizuno T. 2003. The evolutionarily conserved *OsPRR* quintet: rice pseudo-response regulators implicated in circadian rhythm. *Plant Cell Physiol.* 44: 1229-1236.

Nakamichi N, Ito S, Oyama T, Yamashino T, Kondo T, Mizuno T. 2004. Characterization of plant circadian rhythms by employing *Arabidopsis* cultured cells with bioluminescence reporters. *Plant Cell Physiol.* 45: 57–67.

Nakamichi N, Kita M, Ito S, Yamashino, T, Mizuno T. 2005. PSEUDO-RESPONSE REGULATORS, PRR9, PRR7 and PRR5, together play essential roles close to the circadian clock of *Arabidopsis thaliana*. *Plant Cell Physiol.* 46: 686–698.

Nakamichi N, Kita M, Niinuma K, Ito S, Yamashino T, Mizoguchi T, Mizuno T. 2007. *Arabidopsis* clock-associated pseudo-response regulators PRR9, PRR7 and PRR5 coordinately and positively regulate flowering time through the canonical CONSTANS-dependent photoperiodic pathway. *Plant Cell Physiol.* 48: 822-832.

Nakamichi N, Kiba T, Henriques R, Mizuno T, Chua NH, Sakakibara H. 2010. PSEUDO-RESPONSE REGULATORS 9, 7, and 5 are transcriptional repressors in the *Arabidopsis* circadian clock. *Plant Cell* 22: 594-605.

Nishiyama T, Hiwatashi Y, Sakakibara I, Kato M, Hasebe M. 2000. Tagged mutagenesis and gene-trap in the moss, *Physcomitrella patens* by shuttle mutagenesis. *DNA Res.*7: 9–17.

Okada R, Kondo S, Satbhai S.B, Yamaguchi N, Tsukuda M, Aoki A. 2009. Functional characterization of *CCA1*/*LHY* homolog genes, *PpCCA1a* and *PpCCA1b*, in the moss *Physcomitrella patens*. *Plant J.* 60: 551-563.

Onai K, Ishiura M. 2005. PHYTOCLOCK 1 encoding a novel GARP protein essential for the Arabidopsis circadian clock. Genes Cells. 10: 963-72.

Para A, Farre EM, Imaizumi T, Pruneda-Paz JL, Harmon FG, Kay SA. 2007. PRR3 is a vascular regulator of TOC1 stability in the *Arabidopsis* circadian clock. *Plant Cell* 19: 3462–3473.

Park DH, Somers DE, Kim YS, Choy YH, Lim HK, Soh MS, Kim HJ, Kay SA, Nam HG. 1999. Control of circadian rhythms and photoperiodic flowering by the Arabidopsis GIGANTEA gene. *Science*. 285: 1579-82.

Parkinson JS, Kofoid EC. 1992. Communication modules in bacterial signaling proteins. *Annu. Rev. Genet.* 26: 71-112.

Pittendrigh CS. (1993) Temporal organization: reflections of a Darwinian clock-watcher. *Annu. Rev. Physiol.* 55: 16-54.

Plautz JD, Straume M, Stanewsky R, Jamison CF, Brandes C, Dowse HB, Hall JC, Kay SA. 1997. Quantitative analysis of *Drosophila period* gene transcription in living animals. *J. Biol. Rhythms* 12: 204–217.

Prigge MJ and Bezanilla M. 2010. Evolutionary crossroads in developmental biology: Physcomitrella patens. *Development*, 137: 3535-3543.

Ramos A, Pérez-Solís E, Ibáñez C, Casado R, Collada C, Gómez L, Aragoncillo C, Allona I. 2005. Winter disruption of the circadian clock in chestnut. *Proc. Natl. Acad. Sci. USA* 102: 7037-7042.

Rensing SA, Lang D, Zimmer AD, Terry A, Salamov A, Shapiro H, Nishiyama T, Perroud PF, Lindquist EA, Kamisugi Y *et al.* 2008. The *Physcomitrella* genome reveals evolutionary insights into the conquest of land by plants. *Science* 319: 64-69.

Rzhetsky A, Nei M. 1992 A simple method for estimating and testing minimum evolution trees. *Mol. Biol. Evo.* 9: 945-967.

Sambrook, J., Fritsch, E.F., and Maniatis, T. 1989. Molecular Cloning: A Laboratory Manual. (NY: Cold Spring Harbor Laboratory Press).

Satbhai SB, Yamashino T, Okada R, Nomoto Y, Mizuno T, Tezuka Y, Itoh T, Tomita M, Otsuki S, Aoki S. Pseudo-Response Regulator (PRR) Homologues of the Moss Physcomitrella patens: Insights into the Evolution of the PRR Family in Land Plants. *DNA Res*. 2010 Dec 24 (Epub ahead of print).

Sato E, Nakamichi N, Yamashino T, Mizuno T. 2002. Aberrant expression of the Arabidopsis circadian-regulated APRR5 gene belonging to the APRR1/TOC1 quintet results in early flowering and hypersensitiveness to light in early photomorphogenesis. *Plant Cell Physiol*. 43: 1374-85.

Schaefer DG, Zrÿd JP.1997. Efficient gene targeting in the moss *Physcomitrella patens*. *Plant J.* 11: 1195-1206.

Schaffer R, Ramsay N, Samach A, Corden S, Putterill J, Carre IA, and Coupland G. 1998. The late elongated hypocotyl mutation of Arabidopsis disrupts circadian rhythms and the photoperiodic control of flowering. *Cell.* 93: 1219-1229.

Shimizu M, Ichikawa K, Aoki S. 2004. Photoperiod-regulated expression of the PpCOL1 gene encoding a homolog of CO/COL proteins in the moss Physcomitrella patens. *Biochem Biophys Res Commun*. 26: 1296-301.

Somers DE, Schultz TF, Milnamow M, Kay SA. 2000. ZEITLUPE encodes a novel clock-associated PAS protein from Arabidopsis. *Cell*. 101: 319-29.

Southern MM, Brown P, Hall AJW. 2006. Luciferases as reporter genes. *Methods Mol. Biol.* 323: 293–305.

Strayer C, Oyama T, Schultz TF, Raman R, Somers DE, Mas P, Panda S, Kreps JA, and Kay SA. 2000. Cloning of the Arabidopsis clock gene TOC1, an autoregulatory response regulator homolog. *Science*. 289: 768-771.

Sugano S, Andronis C, Green RM, Wang ZY, Tobin EM. 1998. Protein kinase CK2 interacts with and phosphorylates the Arabidopsis circadian clock-associated 1 protein. *Proc Natl Acad Sci U S A*. 95: 11020-5.

Takata N, Saito S, Tanaka-Saito C, Nanjo T, Shinohara K, Uemura M. 2009. Molecular phylogeny and expression of poplar circadian clock genes, *LHY1* and *LHY2*. *New Phytol*. 181: 808-819.

Takata N, Saito S, Satio CT, Uemura M. 2010. Phylogenetic footprint of the plant clock system in angiosperms: evolutionary processes of Pseudo-Response Regulators. *BMC Evol. Biol*. 10: 126.

Tamura K, Dudley J, Nei M, Kumar S. 2007. MEGA4: Molecular Evolutionary Genetics Analysis (MEGA) software version 4.0. *Mol. Biol. Evo.* 24: 1596-1599.

Tsuzuki M, Ishige K, Mizuno T. 1995. Phosphotransfer circuitry of the putative multi-signal transducer, ArcB, of *Escherichia coli*: in vitro studies with mutants. *Mol. Microbiol.* 18: 953-962.

Ueguchi C, Koizumi H, Suzuki T, Mizuno T. 2001. Novel family of sensor histidine kinase genes in *Arabidopsis thaliana*. *Plant Cell Physiol.* 42: 231-235.

Virtudes MR , Uta S, Christopher G,Tim K, Erzsébet F, Ferenc N, Eberhard S, and Klaus H. 2007. Functional cross-talk between two-component and phytochrome B signal transduction in Arabidopsis. *J exp bot*. 58: 2595-2607.

Wang ZY, and Tobin EM. 1998. Constitutive expression of the CIRCADIAN CLOCK ASSOCIATED 1 (CCA1) gene disrupts circadian rhythms and suppresses its own expression. *Cell*. 93: 1207-1217.

Zeilinger MN, Farré EM, Taylor SR, Kay SA, Doyle FJ 3rd. 2006. A novel computational model of the circadian clock in *Arabidopsis* that incorporates PRR7 and PRR9. *Mol. Syst. Biol.* 2:58.